ELSEVIER

INSTITUT PASTEUR

Microbes and Infection 13 (2011) 160–166

www.elsevier.com/locate/micinf

Original article

Effective recognition of HIV-1-infected cells by HIV-1 integrase-specific HLA-B*4002-restricted T cells

Tamayo Watanabe [a,b,1], Hayato Murakoshi [a,1], Hiroyuki Gatanaga [a,b], Madoka Koyanagi [a], Shinichi Oka [a,b,**], Masafumi Takiguchi [a,*]

[a] *Center for AIDS Research, Kumamoto University, 2-2-1 Honjo, Kumamoto 860-0811, Japan*
[b] *AIDS Clinical Center, National Center for Global Health and Medicine, 1-21-1 Toyama, Shinjuku-ku, Tokyo 162-8655, Japan*

Received 1 September 2010; accepted 13 October 2010
Available online 4 November 2010

Abstract

HLA-B*4002 is one of the common HLA-B alleles in the world. All 7 reported HLA-B*4002-restricted HIV epitopes are derived from Gag, Nef, and Vpr. In the present study we sought to identify novel HLA-B*4002-restricted HIV epitopes by using overlapping 11-mer peptides of HIV-1 Nef, Gag, and Pol, and found that 6 of these 11-mer Pol peptides included HLA-B*4002-restricted epitopes. Analysis using truncated peptides of these 6 peptides defined 4 optimal Pol (integrase) epitopes. All epitopes previously reported had Glu at position 2 (P2), suggesting that Glu at P2 is the anchor residue for HLA-B*4002; whereas only 2 of the integrase epitopes that we here identified had Glu at P2. CTL clones specific for the 2 epitopes effectively recognized HIV-1-infected cells whereas those for other 2 epitopes only weakly recognized them. The antigen sensitivity of the former clones for the epitope peptide was much higher than that of the latter clones, suggesting 2 possibilities: 1) the former T cells have high-affinity TCRs and/or 2) the epitope peptides recognized by the former T cells are highly presented by HLA-B*4002 in HIV-1-infected cells. These integrase-specific T cells with high antigen sensitivity may contribute to the suppression of HIV-1 replication in HIV-1-infected HLA-B*4002$^+$ individuals.

Keywords: HIV-1; Cytotoxic T lymphocytes; HLA-B*4002; Integrase

1. Introduction

Human immunodeficiency virus type 1 (HIV-1)-specific cytotoxic T lymphocytes (CTL) play an important role in HIV-1 infections [1–4]. Previous studies demonstrated that HIV-1-specific CTL can inhibit viral replication in vitro [5–7] and that depletion of CD8$^+$ T cells by treatment with an anti-CD8 mAb results in failure of the clearance of the virus in rhesus macaques infected with chimeric simian/human immunodeficiency virus [8]. These studies suggest that the CD8$^+$ CTLs contribute to viral clearance and disease progression in HIV-1-infected individuals. The study of CTL responses in an African cohort demonstrated that HLA-B-restricted T cell responses are associated with lower viral load than HLA-A-restricted or HLA-C-restricted ones [9], suggesting that HLA-B-restricted responses are important for the control of HIV-1. Therefore, the characterization of HIV-1 epitope-specific HLA-B-restricted CTLs is important for understanding the pathogenesis of HIV and developing an AIDS vaccine.

HLA-B*4001 and HLA-B*4002 are common HLA-B alleles in the world. These alleles are found in 10.8% and 16.6% of Japanese population, respectively, and the frequency of HLA-B*4002 is the third highest among HLA-B alleles [10]. Only residue 97 differs between these 2 alleles. So far 10 HLA-B*4001-restricted and 7 HLA-B*4002-restricted HIV epitopes have been reported in Caucasian cohorts [11–16]. These HLA-B*4002-restricted epitopes were derived from

* Corresponding author. Tel.: +81 96 373 6529; fax: +81 96 373 6532.
** Tel./fax: +81 3 5273 5193.
E-mail addresses: oka@acc.ncgm.go.jp (S. Oka), masafumi@kumamoto-u.ac.jp (M. Takiguchi).
[1] Equally contributed.

1286-4579/$ - see front matter © 2010 Institut Pasteur. Published by Elsevier Masson SAS. All rights reserved.
doi:10.1016/j.micinf.2010.10.006

Gag, Nef, and Vpr; whereas the HLA-B*4001-restricted ones came from Gag, Nef, Pol, and Env.

In the present study, we sought to identify HLA-B*4001-restricted and HLA-B*4002-restricted HIV-1 epitopes in chronically HIV-1-infected Japanese cohorts by using 11-mer overlapping peptides derived from Pol, Gag, and Nef. We focused on these 3 proteins in the present study because these major proteins, which provide many CTL epitopes, are considered as vaccine targets. In addition, $CD8^+$ T cell clones specific for these newly identified epitopes were generated and used to clarify their ability to recognize HIV-1-infected cells. In the present study, we found 4 novel integrase epitopes presented by HLA-B*4002 and further characterized the $CD8^+$ T cells specific for these epitopes. Two of these epitopes were considered as immunodominant epitopes, because the specific T cells effectively recognized HIV-1-infected cells.

2. Materials and methods

2.1. Samples of HIV-1-infected individuals

This study was approved by the National Center for Global Health and Medicine and the Kumamoto University Ethical Committee. Informed consent was obtained from all subjects according to the Declaration of Helsinki. Peripheral blood mononuclear cells (PBMCs) were separated from heparinized whole blood. The HLA type of the patients was determined by standard sequence-based genotyping.

2.2. Synthetic peptides

We previously designed and generated overlapping peptides consisting of 11-mer amino acids and spanning Gag, Pol, and Nef of HIV-1 clade B consensus sequences [17]. Each 11-mer peptide was overlapped by 9 amino acids. Truncated peptides of some 11-mer peptides were synthesized by utilizing an automated multiple peptide synthesizer and purified by high-performance liquid chromatography (HPLC). The purity was examined by HPLC and mass spectrometry. Peptides with more than 90% purity were used in the present study.

2.3. Cells

The EBV-transformed B-lymphoblastoid cell lines (B-LCL) were established by transforming B cells from PBMC of KI-400. C1R cells expressing HLA-A*0207 (C1R-A*0207) and those expressing HLA-B*4002 (C1R-B*4002) were generated by transfecting C1R cells with the HLA-A*0207 and HLA-B*4002 genes, respectively. C1R-A*3101 cells were previously generated [18]. 721.221-CD4 cells expressing HLA-B*4002 (.221-CD4-B*4002), HLA-Cw*0102 (.221-CD4-Cw*0102), and HLA-Cw*0304(.221-CD4-Cw*0304) were generated by transfecting 721.221-CD4 cells with the HLA-B*4002, HLA-Cw*0102, and HLA-Cw*0304 genes, respectively, and maintained in RPMI 1640 medium supplemented with 10% FCS and 2.0 mg/ml hygromycin B.

2.4. Intracellular cytokine production (ICC) assay

PBMCs from chronically HIV-1-infected patient KI-400 were stimulated with HIV-1-derived peptide (1 μM) in culture medium (RPMI 1640 medium supplemented with 10% FCS and 200 U/ml recombinant human IL-2). After 14 days in culture, the cells were assessed for IFN-γ production activity by using a FACSCalibur. Briefly, bulk cultures were stimulated with stimulator cells pulsed with HIV-1-derived peptide (1 μM) for 2 h at 37 °C. Brefeldin A (10 μg/ml) was then added, and the cultures were continued for an additional 4 h. Cells were collected and stained with phycoerythrin (PE)-labelled anti-CD8 monoclonal antibody (mAb; Dako Corporation, Glostrup, Denmark). After having been treated with 4% paraformaldehyde solution, the cells were made permeable by incubation in permeabilization buffer (0.1% saponin and 20% NCS in phosphate-buffered saline) at 4 °C for 10 min and then stained with fluorescein isothiocyanate (FITC)-labeled anti-IFN-γ mAb (PharMingen, San Diego, CA). After a thorough washing with the permeabilization buffer, the cells were analyzed by using the FACSCalibur. Similarly IFN-γ production of established CTL clones was analyzed by use of this assay.

2.5. Generation of CTL clones

Peptide-specific CTL clones were generated from established peptide-specific bulk CTLs by seeding 0.8 cells/well into U-bottomed 96-well microtiter plates (Nunc, Roskilde, Denmark) together with 200 μl of cloning mixture (RPMI 1640 medium containing 10% FCS, 200 U/ml human recombinant interleukin-2, 5×10^5 irradiated allogeneic PBMCs from a healthy donor, and 1×10^5 irradiated C1R-B*4002 cells pulsed with a 1 μM concentration of the appropriate HIV-1-derived peptides. Wells positive for growth after about 2 weeks were examined for CTL activity by performing the ICC assay. All CTL clones were cultured in RPMI 1640 containing 10% FCS and 200 U/ml recombinant human interleukin-2. CTL clones were stimulated biweekly with irradiated target cells pulsed with the corresponding peptides.

2.6. HIV-1 clones

NL-432, which is an infectious proviral clone of HIV-1, was previously reported [7,19].

2.7. HIV-1 infection of .221-CD4-B*4002 and .221-CD4 cells

.221-CD4-B*4002 and 721.221-CD4 cells were exposed to NL-432 for several days. These infected cells were used as stimulator cells for ICC assays when approximately 60% of cells had been infected, which was confirmed by intracellular staining for HIV-1 p24 antigen.

3. Results

*3.1. Identification of 11-mer peptides recognized by HLA-B*4001-restricted and HLA-B*4002-restricted HIV-1-specific CD8$^+$ T cells*

To identify novel HLA-B*4001-restricted CTL epitopes, we analyzed 5 HIV-seropositive HLA-B*4001$^+$ Japanese individuals by Elispot assays with cocktails of overlapping 11-mer peptides spanning Gag (p17^{Gag}, p24^{Gag}, p2p7p1p6^{Gag}), Pol (Protease, RT, integrase), and Nef. The overlapping 11-mer peptide cocktails that gave more than 200 spots per 10^6 cells were used to stimulate PBMC of each patient in order to identify the epitopes. After the PBMC had been cultured for 2 weeks, their IFN-γ production was analyzed by using the ICC assay. We found that 3 peptide cocktails induced IFN-γ production. Further analysis using 10 peptides in the peptide cocktails showed that three 11-mer peptides included HLA-B*4001-restricted epitopes but all of these peptides contained reported HLA-B*4001-restricted epitope sequences. Thus, we could not find any novel HLA-B*4001-restricted epitopes.

In order to identify CTL epitopes restricted by HLA-B*4002, we analyzed fresh CD8$^+$ T cells from patient KI-400 (A*0207/A*3101, B*4002/B*4601, Cw*0102/Cw*0304) by performing Elispot assays with the cocktails of the overlapping 11-mer peptides. More than 200 spots per 10^6 cells were observed with 7 out of 25 Gag cocktails, 11 out of 50 Pol cocktails, and 1 out of 10 Nef cocktails (data not shown). To find novel HLA-B*4002-restricted CTL epitopes, we focused on analyzing 5 peptide cocktails (Gag21-49, Pol781-809, Pol801-829, Pol901-929, and Pol921-949) that did not contain reported epitopes restricted by the 6 HLA-class I alleles this patient expressed. To determine which peptide in each cocktail induced the specific CD8$^+$ T cells, we stimulated PBMCs from KI-400 with these peptide cocktails and then cultured the cells for 2 weeks. The responsiveness of the cultured CD8$^+$ T cells toward ten 11-mer peptides in each peptide cocktail was measured by using the ICC assay. IFN-γ production was found in the bulk CD8$^+$ T cells stimulated with autologous B-LCLs pre-pulsed with 2 Gag (Gag31-41 and Gag33-43) and 6 Pol peptides (Pol799-809, Pol807-817, Pol909-919, Pol911-921, Pol919-929, and Pol921-931).

For determination of HLA restriction molecules of CD8$^+$ T cells specific for these 11-mer peptides, the responsiveness of the bulk CD8$^+$ T cells towards peptide-pulsed C1R cells expressing one of the HLA-A or -B alleles or .221 cells expressing one of the HLA-C alleles was measured by performing the ICC assay. HLA-B*4002-restricted responses were found in the bulk culture cells stimulated with the cells pre-pulsed with Pol799-809, Pol807-817, Pol909-919, Pol911-921, Pol919-929 or Pol921-931 (data not shown). These results indicate that these six 11-mer peptides included HLA-B*4002-restricted epitopes.

*3.2. Identification of HLA-B*4002-restricted optimal epitope peptides*

To determine the optimal epitopes for these 11-mer peptides, we stimulated bulk T cells with C1R-B*4002 cells pre-pulsed with truncated peptide of Pol799-809, Pol807-817, Pol909-919, Pol911-921, Pol919-929 or Pol921-931 at concentrations of 1000 nM and then measured the IFN-γ production of each bulk T cells was measured by conducting the ICC assay. Previous studies on HLA-B*4002-restricted epitopes suggested that Glu at position 2 is an anchor for HLA-B*4002 (11–16). Judging from the finding that Pol801-811 did not include HLA-B*4002-restricted epitopes, we speculated that 2E in Pol799-809 (IG11: IEAEVIPAETG) would be the anchor for HLA-B*4002 rather than 4E. We therefore generated 5 truncated peptides (IT10: IEAEVIPAET, IA8: IEAEVIPA, ET9: EAEVIPAET, AT8: AEVIPAET, and AG9: AEVIPAETG) of Pol799-809 and investigated whether CD8$^+$ T cells induced by Pol799-809 would recognize these peptides. The T cells recognized only IG11 and IT10 at 1000 nM (Fig. 1A), whereas they showed higher sensitivity to IT10 than to IG11 (Fig. 1B). These findings indicate that Pol799-808 (IT10) was the optimal epitope.

For Pol807-817 (EL11: ETGQETAYFLL), we generated 4 truncated peptides (TL10: TGQETAYFLL, GL9: GQETAYFLL, GL8: GQETAYFL, and QL8: QETAYFLL). CD8$^+$ T cells induced by the Pol807-817 peptide recognized EL11, TL10, GL9 and QL8, but not GL8 (Fig. 1A), indicating that L at position 11 was critical for the epitope. On the other hand, the T cells showed higher sensitivity to EL11 than to the other 3 peptides (Fig. 1C). These findings indicate that Pol807-817 (EL11) was the optimal epitope.

For Pol909-919 (YI11: YSAGERIVDII) and Pol911-921 (AT11: AGERIVDIIAT), we assumed 2 possibilities: 1) the two 11-mer peptides shared the same epitope, or 2) the two peptides included different epitopes. To clarify these possibilities, we analyzed Pol909-919 and Pol911-921 independently. For Pol909-919, we generated 5 truncated peptides (SI10: SAGERIVDII, SI9: SAGERIVDI, AI8: AGERIVDI, AI9: AGERIVDII, and GI8: GERIVDII). CD8$^+$ T cells induced by Pol909-919 peptide recognized YI11, SI10, AI9, and GI8, but not SI9 and AI8 (Fig. 1A), indicating that I at position 11 was critical for this epitope. On the other hand, they showed higher sensitivity to GI8 than to the other 3 peptides (Fig. 1D). These findings indicate that Pol909-919 (GI8) was the optimal epitope. Regarding Pol911-921 (AT11), we generated 4 truncated peptides (AI9: AGERIVDII, AI8: AGERIVDI, GI8: GERIVDII, and GA9: GERIVDIIA). CD8$^+$ T cells induced by Pol911-921 peptide recognized AT11, AI9, GI8 and GA9, but not AI8 (Fig. 1A), indicating I at position 11 to be critical for this epitope. They also showed higher sensitivity to GI8 than to the other 3 peptides (Fig. 1E), indicating that GI8 (Pol912-919) was the optimal epitope. Thus, these results confirmed that Pol909-919 and Pol911-921 included the same epitope.

For Pol919-929 (IQ11: IATDIQTKELQ) and Pol921-931 (TQ11: TDIQTKELQKQ), we assumed that these two 11-mer peptides shared the same epitope. Therefore, we analyzed Pol919-929 and Pol921-931 independently. Regarding Pol919-929 (IQ11: IATDIQTKELQ) we speculated that 10L would be the C-terminus of the epitope because no hydrophilic residue is found in the C-terminus of HLA class I-binding peptides.

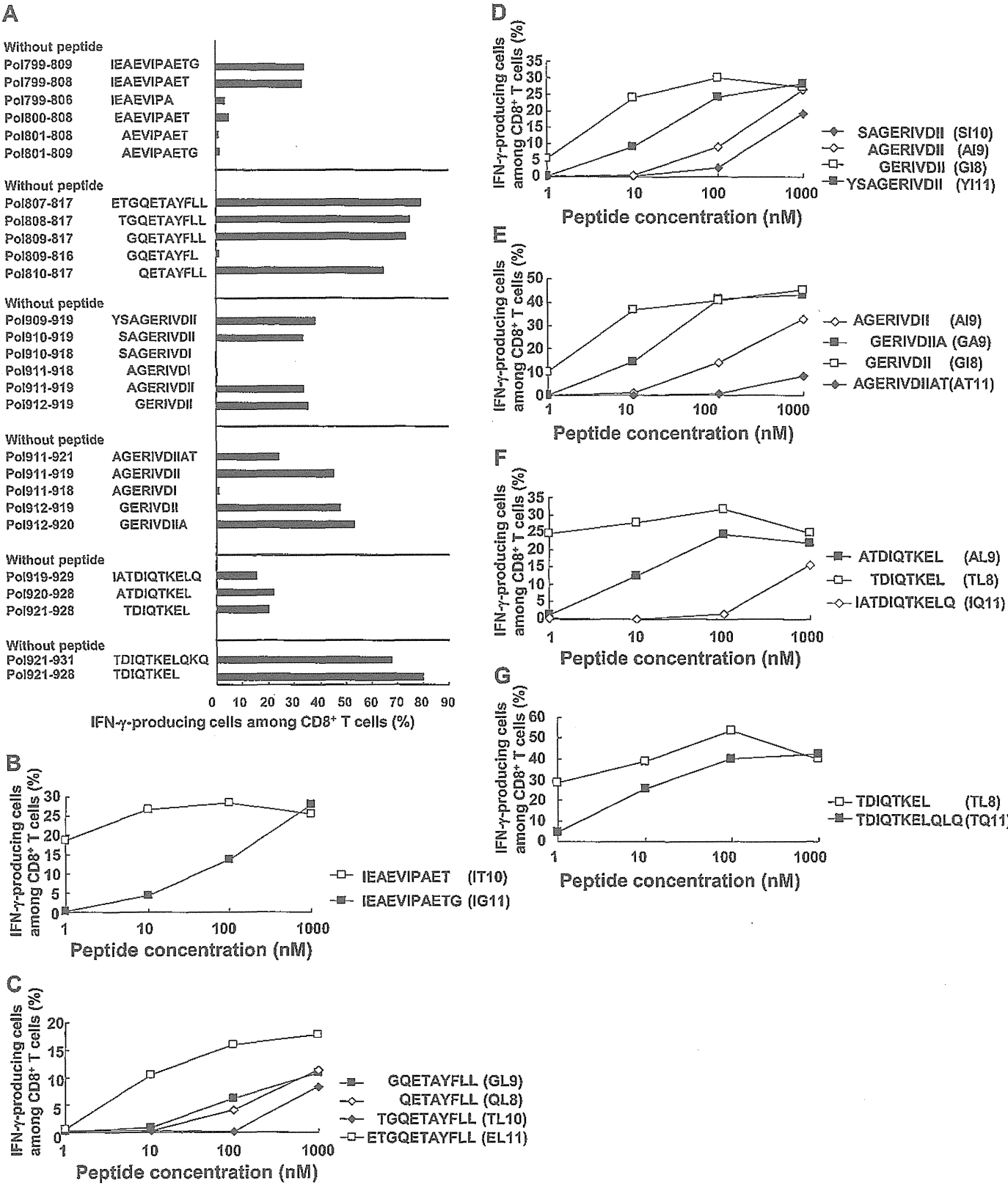

Fig. 1. Identification of HLA-B*4002-restricted HIV-1 CTL epitopes. A. For determination of the optimal epitopes of Pol799-809, Pol807-817, Pol909-919, Pol911-921, Pol919-929 and Pol921-931, the recognition of the bulk T cells for the truncated peptides was examined by using C1R-B*4002 cells pre-pulsed with each truncated peptide at a concentration of 1000 nM. The responsiveness of the bulk $CD8^+$ T cells toward each truncated peptide was measured by using the ICC assay. The percentages of IFN-γ-producing cells among the $CD8^+$ T cells are shown in the figure. B–G. Optimal epitopes were not determined at concentrations of 1000 nM for Pol799-809 (B), Pol807-817 (C), Pol909-919 (D), Pol911-921 (E), Pol919-929 (F) or Pol921-931 (G). The responsiveness of the bulk $CD8^+$ T cells was examined for C1R-B*4002 cells pre-pulsed with each truncated peptide at concentrations from 1 to 1000 nM. The responsiveness of the bulk $CD8^+$ T cells toward each truncated peptide was measured by performing the ICC assay. The percentages of IFN-γ-producing cells among $CD8^+$ T cells are shown in the figure.

Therefore, we generated 2 truncated peptides (AL9: ATDIQTKEL and TL8: TDIQTKEL). Bulk $CD8^+$ T cells induced by Pol919-929 peptide recognized all 3 peptides (Fig. 1A) and showed higher sensitivity to TL8 than to the other 2 peptides (Fig. 1F), indicating that Pol921-928 (TL8) was the optimal epitope. Similarly we speculated TL8 to be optimal epitope for Pol921-931 (TQ11: TDIQTKELQKQ), because no hydrophilic residue is found in the C-terminus of HLA-class I-restricted epitopes. Although bulk $CD8^+$ T cells induced by Pol921-931 peptide recognized both TQ11 and TL8 peptides (Fig. 1A), they showed higher sensitivity to TL8 than to TQ11 (Fig. 1F). These findings indicate that Pol919-929 and Pol921-931 11-mer peptides included the same epitope, Pol921-928(TL8).

Thus, we identified 4 HLA-B*4002-restricted optimal peptides. Interestingly, these 4 Pol epitopes were all derived from integrase.

*3.3. Generation and antigen sensitivity of HLA-B*4002-restricted Pol-specific CTL clones*

To analyze the $CD8^+$ T cells specific for these 4 integrase epitopes, IT10 (Pol799-808), EL11 (Pol807-817), GI8 (Pol912-919), and TL8 (Pol921-928), we established the specific $CD8^+$ T cell clones and analyzed them for their antigen sensitivity by using the ICC assays. The result was shown in Fig. 2. The T cell clones and their EC_{50} values were as follows: Pol799-808-specific T cells (27.7), Pol807-817-specific T cells (191.7), Pol912-919-specific T cells (443.1), and Pol921-928-specific T cells (7.6). These results indicate that Pol799-808-specific and Pol921-928-specific $CD8^+$ T cell clones had higher antigen sensitivity than Pol807-817-specific and Pol912-919-specific ones.

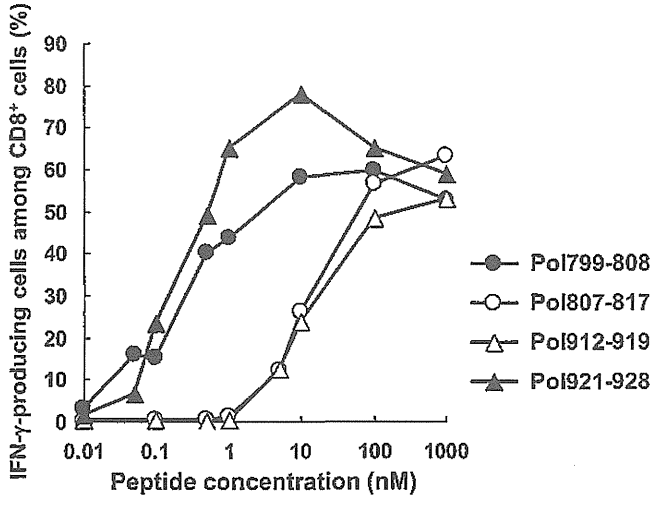

Fig. 2. Antigen Sensitivity of 4 HIV-1 integrase-specific $CD8^+$ T cells. Antigen sensitivity of 4 HIV-1 integrase-specific $CD8^+$ T cells was examined by using the ICC assay. The responsiveness of these CTL clones was examined for C1R-B*4002 cells pre-pulsed with each truncated peptide at concentrations from 0.01 to 1000 nM.

3.4. Recognition of HIV-1-infected cells by specific T cells

To clarify whether Pol799-808, Pol807-817, Pol912-919, and Pol921-928 were naturally occurring peptides and whether CTLs specific for these epitopes had the ability to recognize HIV-1-infected cells, we investigated the response of these peptide-specific $CD8^+$ T cell clones toward HIV-1 (NL-432)-infected .221-CD4 cell lines expressing HLA-B*4002. NL-432 includes wild-type sequences of these 4 epitopes. .221-CD4 cell lines and those expressing HLA-B*4002 were infected with NL-432, and then cultured for 4 days. The responses of the T cell clones toward these infected cells were measured by using the ICC assay. The percentage of the HIV-1-infected cells was determined by staining intracellular HIV-1 p24 (Fig. 3A). The Pol799-808-specific, Pol807-817-specific, Pol912-919-specific, and Pol921-928-specific CTL clones responded to .221-CD4-B*4002 cells infected with HIV-1 but not to uninfected .221-CD4-B*4002 cells or to HLA-B*4002-negative .221-CD4 cells infected with HIV-1. These results indicate that Pol799-808, Pol807-817, and Pol921-928 peptides were naturally processed and presented by HLA-B*4002 and that the T cells specific for these epitopes could recognize HIV-1-infected cells (Fig. 3B). On the other hand, the responses of Pol807-817-specific and Pol912-919-specific CTL clones was much weaker than those of the other CTL clones (Fig. 3B), indicating that the former CTLs only weakly recognized HIV-1-infected cells.

4. Discussion

There is only 1 amino acid substitution, at residue 97, on the peptide binding floor between HLA-B*4001 and HLA-B*4002. A previous study on the peptide motif of HLA-B*4001 showed that HLA-B*4001-binding peptide anchors are Glu at P2 (2E) and Leu at the C-terminus [20]. Indeed, 7 of 8 reported HLA-B*4001-restricted HIV-1-specific T cell epitopes have 2E and Leu at their C-terminus [11–13]. Although no HLA-B*4002-binding peptide motif had not yet been identified, we speculated that this motif would be similar to the HLA-B*4001-binding one. Indeed, all 7 HLA-B*4002-restricted epitopes previously reported have 2E (Table 1). However, 2 of the 4 epitopes identified in the present study did not have the 2E anchor. In addition, only 5 of 11 HLA-B*4002-restricted epitopes had Leu at their C-terminus. These findings suggest that the substitution from Ser to Arg at residue 97 may partially affect the structure of the F and B pockets. Pol807-817 (ETGQETAYFLL) does not have the 2E anchor. QL8 (QETAYFLL) is speculated to be an HLA-B*4002-restricted epitope because this peptide has 2E. However, the antigen sensitivity of the T cells specific for QL8 is much weaker than that for EL11. This result excludes the possibility that QL8 is the epitope peptide. Thr at position 2 of Pol807-817 may bind to the residues facing the B-pocket by hydrogen-bonding. Nine of the 11 HLA-B*4002-restricted epitopes have 2E, suggesting that the 2E is still anchor residue for HLA-B*4002.

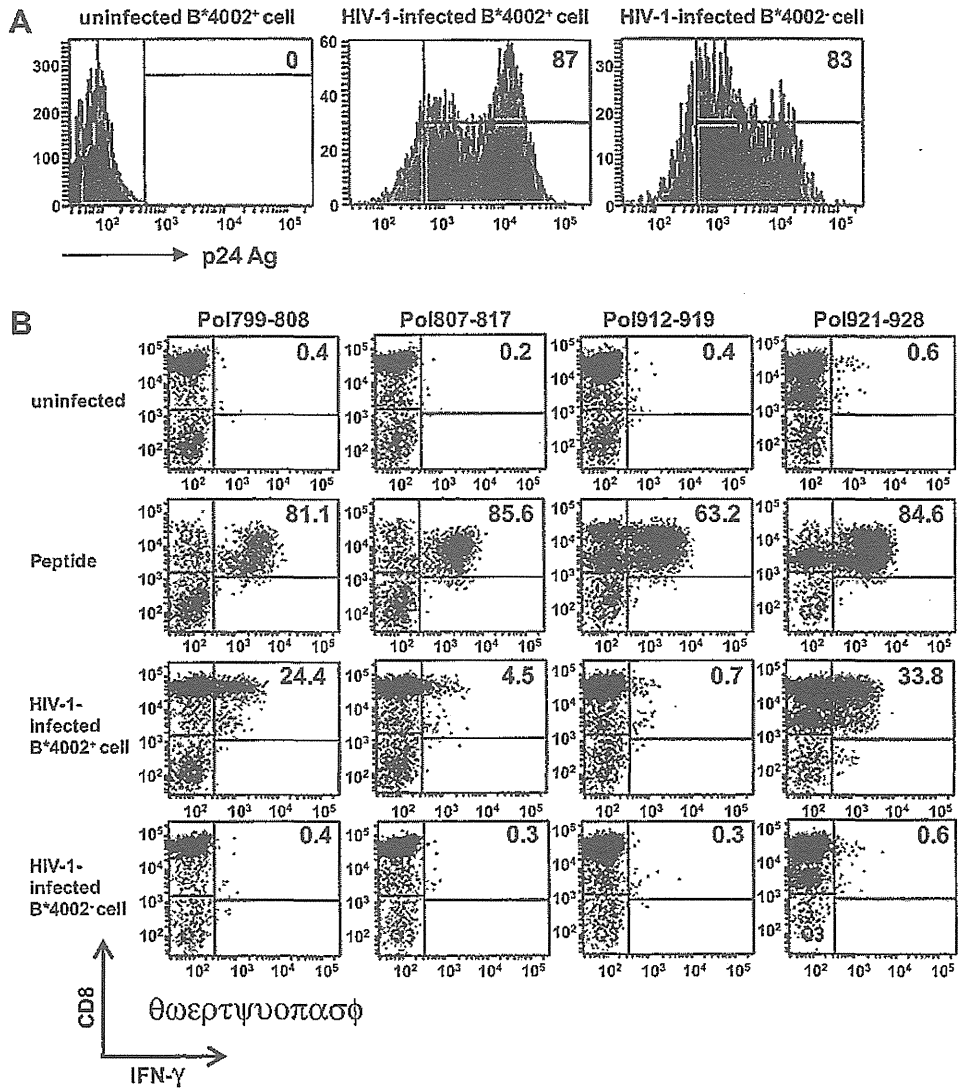

Fig. 3. Ability of 4 HIV-1 integrase-specific $CD8^+$ T cells to recognize HIV-1-infected cells. A. The .221-CD4 and $B*4002^+$.221-CD4 cell lines were infected with HIV-1 (NL-432) and cultured for 4 days. The frequency of HIV-1-infected cells was detected by using staining of intracellular p24 with anti-p24 mAb. The percentage of HIV-1-infected cells is shown in each figure. B. Recognition of HIV-1-infected cells by the Pol799-808-, Pol807-817-, Pol912-919- or Pol921-928-specific $CD8^+$ T cell clones. The activities of these peptide-specific $CD8^+$ T cell clones to recognize $B*4002^+$.221-CD4 cell lines infected with HIV-1 or those pre-pulsed with the corresponding peptide (1000 nM) were measured by use of the ICC assay. The percentages of IFN-γ-producing cells among $CD8^+$ T cells are shown in each figure.

Although the 7 HLA-B*4002-restricted epitopes previously reported do not include Pol-derived ones, we identified novel 4 HLA-B*4002-retricted Pol-specific T cell epitopes in the present study. Interestingly, all of these Pol epitopes were derived from integrase. Though 29 integrase epitopes were reported as 20 different HLA class I-restricted epitopes (Los Alamos HIV Molecular Immunology Data), integrase epitopes were not found among HLA-B*4001-restricted Pol epitopes. Regarding the integrase epitopes, HLA-B*4201 and HLA-B*1503 present 3 different epitopes, whereas the other 18 alleles present 1 or 2 epitopes. Thus, HLA-B*4002 is so far the only HLA-class I allele that can present more than 3 integrase epitopes.

Pol799-808-specific and Pol921-928-specific T cells strongly recognized HIV-1-infected cells, whereas Pol807-817-specific and Pol912-919-specific ones weakly recognized these cells. Antigen sensitivity of the former T cells was much higher than that of the latter ones. Thus, the ability to recognize HIV-1-infected cells was associated with the antigen sensitivity. However, it is difficult to clarify why the 2 T cells weakly recognize HIV-1-infected cells because we did not measure the bindings of these epitope peptides to HLA-B*4002 molecules and of the specific tetramers to the specific T cells. We can suggest 2 possibilities from the data shown in Fig. 2 and Fig. 3: 1) The former T cells may have higher affinity TCR and/or 2) these former epitope peptides are more highly presented than the latter by HLA-B*4002 in HIV-1-infected cells. Since Pol799-808-specific and Pol921-928-specific T cells strongly recognized HIV-1-infected cells, we proposed that they would effectively recognize and kill HIV-1-infected cells *in vivo*.

HLA-B*4001 and HLA-B*4002 are found in 10.8% and 16.6% of the Japanese population, respectively. Since both

Table 1
A list of HLA-B*4002-restricted epitopes identified previously and in this study.

Sequence	Protein	Reference
GELDRWEKI	Gag (p17)	*15
KETINEEAA	Gag (p24)	*15
AEWDRVHPV	Gag (p24)	*15
AEAMSQVTNS	Gag (p2p7p1p6)	*16
TERQANFL	Gag (p2p7p1p6)	*15
REPHNEWTL	Vpr	*14
KEKGGLEGL	Nef	*15
IEAEVIPAET	Pol (Integrase)	This study (Pol799-808)
ETGQETAYFLL	Pol (Integrase)	This study (Pol807-817)
GERIVDII	Pol (Integrase)	This study (Pol912-919)
TDIQTKEL	Pol (Integrase)	This study (Pol921-928)

HLA-class I alleles are detected in approximately 25% of Japanese individuals, T cell epitopes presented by these alleles are useful for studies on HIV-1 immunopathogenesis and the development of AIDS vaccines.

Acknowledgments

The authors thank Sachiko Sakai for secretarial assistance. This research was supported by the Program of Founding Research Centers for Emerging and Reemerging Infectious Diseases and by the Global COE program "Global Education and Research Center Aiming at the control of AIDS" supported by the Ministry of Education, Science, Sports and Culture, Japan; by a grant-in-aid (No. 20390134) for scientific research from the Ministry of Health, Japan; and by a grant-in-aid (No. 18390141) for scientific research from the Ministry of Education, Science, Sports and Culture, Japan.

References

[1] R.A. Koup, J.T. Safrit, Y. Cao, C.A. Andrews, G. McLeod, W. Borkowsky, C. Farthing, D.D. Ho, Temporal association of cellular immune responses with the initial control of viremia in primary human immunodeficiency virus type 1 syndrome, J. Virol. 68 (1994) 4650–4655.

[2] G. Pantaleo, J.F. Demarest, H. Soudeyns, C. Graziosi, F. Denis, J.W. Adelsberger, P. Borrow, M.S. Saag, G.M. Shaw, P.S. Sekaly, A.S. Fauci, Major expansion of $CD8^+$ T cells with a predominant Vβ usage during the primary immune response to HIV, Nature 370 (1994) 463–467.

[3] P.A. Moss, S.L. Rowland-Jones, P.M. Frodsham, S. McAdam, P. Giangrande, A.J. McMichael, J.I. Bell, Persistent high frequency of human immunodeficiency virus-specific cytotoxic T cells in peripheral blood of infected donors, Proc. Natl. Acad. Sci. U S A 92 (1995) 5773–5777.

[4] S. Rowland-Jones, J. Sutton, K. Ariyoshi, T. Dong, F. Gotch, S. McAdam, D. Whitby, S. Sabally, A. Gallimore, T. Corrah, M. Takiguchi, T. Schultz, A. McMichael, H. Whittle, HIV-1 specific cytotoxic T cells in HIV-exposed but uninfected Gambian women, Nat. Med. 1 (1995) 59–64.

[5] C.M. Walker, D.J. Moody, D.P. Stites, J.A. Levy, $CD8^+$ lymphocytes can control HIV infection in vitro by suppressing virus replication, Science 234 (1986) 1563–1566.

[6] O.O. Yang, B.D. Walker, $CD8^+$ cells in human immunodeficiency virus type I pathogenesis: cytolytic and noncytolytic inhibition of viral replication, Adv. Immunol. 66 (1997) 273–311.

[7] H. Tomiyama, H. Akari, A. Adachi, M. Takiguchi, Different effects of Nef-mediated HLA class I down-regulation on human immunodeficiency virus type 1-specific $CD8^+$ T-cell cytolytic activity and cytokine production, J. Virol. 76 (2002) 7535–7543.

[8] T. Matano, R. Shibata, C. Siemon, M. Connors, H.C. Lane, M.A. Martin, Administration of an anti-CD8 monoclonal antibody interferes with the clearance of chimeric simian/human immunodeficiency virus during primary infections of rhesus macaques, J. Virol. 72 (1998) 164–169.

[9] P. Kiepiela, A.J. Leslie, I. Honeyborne, D. Ramduth, C. Thobakgale, S. Chetty, P. Rathnavalu, C. Moore, K.J. Pfafferott, L. Hilton, P. Zimbwa, S. Moore, T. Allen, C. Brander, M.M. Addo, M. Altfeld, I. James, S. Mallal, M. Bunce, L.D. Barber, J. Szinger, C. Day, P. Klenerman, J. Mullins, B. Korber, H.M. Coovadia, B.D. Walker, P.J. Goulder, Dominant influence of HLA-B in mediating the potential co-evolution of HIV and HLA, Nature 432 (2004) 769–775.

[10] Y. Itoh, N. Mizuki, T. Shimada, F. Azuma, M. Itakura, K. Kashiwase, E. Kikkawa, J.K. Kulski, M. Satake, H. Inoko, High-throughput DNA typing of HLA-A, -B, -C, and -DRB1 loci by a PCR-SSOP-Luminex method in the Japanese population, Immunogenetics 57 (2005) 717–729.

[11] M.A. Altfeld, A. Trocha, R.L. Eldridge, E.S. Rosenberg, M.N. Phillips, M.M. Addo, R.P. Sekaly, S.A. Kalams, S.A. Burchett, K. McIntosh, B.D. Walker, P.J. Goulder, Identification of dominant optimal HLA-B60- and HLA-B61-restricted cytotoxic T-lymphocyte (CTL) epitopes: rapid characterization of CTL responses by enzyme-linked immunospot assay, J. Virol. 74 (2000) 8541–8549.

[12] X.G. Yu, H. Shang, M.M. Addo, R.L. Eldridge, M.N. Phillips, M.E. Feeney, D. Strick, C. Brander, P.J. Goulder, E.S. Rosenberg, B.D. Walker, M. Altfeld, Important contribution of p15 Gag-specific responses to the total Gag-specific CTL responses, AIDS 16 (2002) 321–328.

[13] R. Draenert, T.M. Allen, Y. Liu, T. Wrin, C. Chappey, C.L. Verrill, G. Sirera, R.L. Eldridge, M.P. Lahaie, L. Ruiz, B. Clotet, C.J. Petropoulos, B.D. Walker, J. Martinez-Picado, Constraints on HIV-1 evolution and immunodominance revealed in monozygotic adult twins infected with the same virus, J. Exp. Med. 203 (2006) 529–539.

[14] M. Altfeld, M.M. Addo, R.L. Eldridge, X.G. Yu, S. Thomas, A. Khatri, D. Strick, M.N. Phillips, G.B. Cohen, S.A. Islam, S.A. Kalams, C. Brander, P.J. Goulder, E.S. Rosenberg, B.D. Walker, Vpr is preferentially targeted by CTL during HIV-1 infection, J. Immunol. 167 (2001) 2743–2752.

[15] S. Sabbaj, A. Bansal, G.D. Ritter, C. Perkins, B.H. Edwards, E. Gough, J. Tang, J.J. Szinger, B. Korber, C.M. Wilson, R.A. Kaslow, M.J. Mulligan, P.A. Goepfert, Cross-reactive CD8+ T cell epitopes identified in US adolescent minorities, J. Acquir. Immune. Defic. Syndr. 33 (2003) 426–438.

[16] T. Bhattacharya, M. Daniels, D. Heckerman, B. Foley, N. Frahm, C. Kadie, J. Carlson, K. Yusim, B. McMahon, B. Gaschen, S. Mallal, J.I. Mullins, D.C. Nickle, J. Herbeck, C. Rousseau, G.H. Learn, T. Miura, C. Brander, B. Walker, B. Korber, Founder effects in the assessment of HIV polymorphisms and HLA allele associations, Science 315 (2007) 1583–1586.

[17] H. Murakoshi, M. Kitano, T. Akahoshi, Y. Kawashima, S. Dohki, S. Oka, M. Takiguchi, Identification and characterization of 2 HIV-1 Gag immunodominant epitopes restricted by Asian HLA allele HLA-B*4801, Hum. Immunol. 70 (2009) 170–174.

[18] M.A. Borghan, S. Oka, M. Takiguchi, Identification of HLA-A*3101-restricted cytotoxic T-lymphocyte response to human immunodeficiency virus type 1 (HIV-1) in patients with chronic HIV-1 infection, Tissue Antigens 66 (2005) 305–313.

[19] H. Akari, S. Arold, T. Fukumori, T. Okazaki, K. Strebel, A. Adachi, Nef-induced major histocompatibility complex class I down-regulation is functionally dissociated from its virion incorporation, enhancement of viral infectivity, and CD4 down-regulation, J. Virol. 74 (2000) 2907–2912.

[20] K. Falk, O. Rotzschke, M. Takiguchi, V. Gnau, S. Stevanovic, G. Jung, H.G. Rammensee, Peptide motifs of HLA-B58, B60, B61, and B62 molecules, Immunogenetics 41 (1995) 165–168.

AIDS RESEARCH AND HUMAN RETROVIRUSES
Volume 27, Number 10, 2011

DOI: 10.1089/aid.2010.0196

Identification of a Current Hot Spot of HIV Type 1 Transmission in Mongolia by Molecular Epidemiological Analysis

Jagdagsuren Davaalkham,[1,2] Puntsag Unenchimeg,[3] Chultem Baigalmaa,[3] Gombo Erdenetuya,[3] Dulmaa Nyamkhuu,[3] Teiichiro Shiino,[4] Kiyoto Tsuchiya,[1] Tsunefusa Hayashida,[1,2] Hiroyuki Gatanaga,[1,2] and Shinichi Oka[1,2]

Abstract

We investigated the current molecular epidemiological status of HIV-1 in Mongolia, a country with very low incidence of HIV-1 though with rapid expansion in recent years. HIV-1 *pol* (1065 nt) and *env* (447 nt) genes were sequenced to construct phylogenetic trees. The evolutionary rates, molecular clock phylogenies, and other evolutionary parameters were estimated from heterochronous genomic sequences of HIV-1 subtype B by the Bayesian Markov chain Monte Carlo method. We obtained 41 sera from 56 reported HIV-1-positive cases as of May 2009. The main route of infection was men who have sex with men (MSM). Dominant subtypes were subtype B in 32 cases (78%) followed by subtype CRF02_AG (9.8%). The phylogenetic analysis of the *pol* gene identified two clusters in subtype B sequences. Cluster 1 consisted of 21 cases including MSM and other routes of infection, and cluster 2 consisted of eight MSM cases. The tree analyses demonstrated very short branch lengths in cluster 1, suggesting a surprisingly active expansion of HIV-1 transmission during a short period with the same ancestor virus. Evolutionary analysis indicated that the outbreak started around the early 2000s. This study identified a current hot spot of HIV-1 transmission and potential seed of the epidemic in Mongolia. Comprehensive preventive measures targeting this group are urgently needed.

Introduction

MONGOLIA HAS A LOW PREVALENCE of HIV with estimated infected individuals comprising less than 0.01% of the general population. However, this number is increasing rapidly and recent statistical data estimated a 10-fold increase in HIV/AIDS incidence during the past 5 years. Since 1992, when data on HIV/AIDS began to be compiled in Mongolia, there had been only five cases reported as of December 2004. In 2005, the number of infected cases increased sharply and 11 cases were registered in that year. According to an unpublished report from the Ministry of Health Mongolia, the total number of HIV infected cases was 56 as of May 2009. The infected individuals were men who have sex with men (MSM) 64.3%, heterosexual males (HSM) 14.3%, and females (HSF) 21.4%, of whom 50% were female sex workers (FSW).

The Second Generation HIV/Sexually Transmitted Infections (STI) surveillance program (SGS) for HIV/STI serological studies in various behaviors was initiated in Mongolia in 2002. According to the latest results of the SGS conducted in 2007, the HIV prevalence among blood donors and pregnant women was zero and among 1350 tuberculosis patients was 0.15% (95% CI 0.00–0.35).[1] The results of our 2007 prevalence survey of 2465 individuals (1415 high-risk and 1050 healthy control populations) in Mongolia demonstrated that the current HIV prevalence is low, but according to the high prevalence of syphilis (anti-TP 23.1%) and HCV (anti-HCV 8%) in high-risk populations, the risk status for HIV-1 infection is estimated to be high.[2] The high-risk populations included FSW, MSM, mobile men, tuberculosis (TB) patients, and male STI clinic clients; healthy control populations were youth and blood donors.

Knowledge about current patterns and trends of HIV infections is essential for planning and evaluating prevention programs and for resource allocation. In the past, epidemiological data on newly diagnosed HIV/AIDS and results of a

[1]AIDS Clinical Center, National Center for Global Health and Medicine, Tokyo, Japan.
[2]Division of Infectious Diseases, Center for AIDS Research, Kumamoto University, Kumamoto, Japan.
[3]National Center for Communicable Diseases, Ministry of Health, Ulaanbaatar, Mongolia.
[4]National Institute of Infectious Diseases, Tokyo, Japan.

surveillance study of HIV/STI have been used for planning and targeting HIV prevention programs in Mongolia. However, these data were not sufficient to implement a comprehensive, effective, targeted strategy for prevention of HIV infection in Mongolia. To gain a better understanding of the current HIV status, a more detailed molecular epidemiological study using phylogenetic analyses is needed. Molecular epidemiological analyses are useful tools to gain information about the origin of HIV epidemics and transmission patterns.[3,4] Moreover, information regarding the genetic diversity of HIV strains, and the geographic prevalence of genotypes, is important for the evaluation of diagnostic tests and vaccines and for their effective application.[5,6]

In the present study, we used phylogenetic analyses to determine the HIV-1 subtypes circulating in Mongolia, especially the dominant subtypes responsible for the outbreak in the infected population. Then, we performed a Bayesian coalescent-based framework to investigate the origin and estimate the onset year of the dominant HIV-1 subtypes in Mongolia.

Materials and Methods

Study population

After obtaining informed consent, blood samples were collected anonymously from 39 Mongolian HIV-1-positive patients attending the National Center for Communicable Diseases of Mongolia (NCCD) in November 2007 and May 2009. For all of them, HIV infection was diagnosed from 1997 to 2009, and all participants were infected through sexual contact. In this study, we also examined two stored serum samples at the NCCD obtained from a Russian married couple who were diagnosed with HIV-1 in Mongolia in 2007. Therefore, a total of 39 (69.6%) samples out of all 56 reported cases in Mongolia as of May 2009 was examined in this study. The study subjects were 32 men [mean age (±SD): 31.3±7.8 years, range: 17–52 years] and 9 females (25.9±5.1, 18–33 years) and 63.4% of them had a high level (college/university) of education (Table 1). The *StatView* software version 5.0 (SAS Institute, Cary, NC) was used for statistical analyses. The collected serum samples were sent to the AIDS Clinical Center, National Center for Global Health and Medicine (NCGM), Tokyo, Japan, for further analysis. The study protocol was approved by the ethics committees of NCGM (H19-448 and H20-545) and the Ministry of Health, Mongolia (2007-#7 and 2008-#3).

Table 1. Epidemiological Characteristics of the 41 HIV-1 Infected Patients

Characteristics	*Male (%)*	*Female (%)*
Gender	32 (78)	9 (22)
Age groups (based on age at first diagnosis)		
<20	1 (2.4)	1 (2.4)
20–29	15 (36.6)	5 (12.2)
30–39	10 (24.4)	2 (4.9)
40–49	4 (9.8)	0 (0)
>50	1 (2.4)	0 (0)
Unknown	1 (2.4)	1 (2.4)
Ethnicity		
Mongolian	31 (75.6)	8 (19.5)
Russian	1 (2.4)	1 (2.4)
Transmission category		
Homosexual	27 (65.8)	0 (0)
Heterosexual	4 (9.8)	9 (22)[a]
Unknown	1 (2.4)	0 (0)
Education		
Uneducated	1 (2.4)	0 (0)
Primary	0 (0)	0 (0)
Incomplete secondary	2 (4.9)	3 (7.3)
Complete secondary	5 (12.2)	2 (4.9)
College/university	23 (56.1)	3 (7.3)
Unknown	1 (2.4)	1 (2.4)
HIV-1 subtype		
B	30 (73.1)	2 (4.9)
C	0 (0)	2 (4.9)
G	2 (4.9)	0 (0)
CRF01_AE	0 (0)	1 (2.4)
CRF02_AG	0 (0)	4 (9.8)

[a]Five (55.6%) of the female cases were female sex workers.

Amplification and sequencing of HIV-1

Total RNA was extracted from 140 μl of serum, using the QIAamp RNA Mini Kit (Qiagen, Valencia, CA) according to the instructions supplied by the manufacturer. HIV-1 cDNA was obtained by reverse transcriptase polymerase chain reaction (RT-PCR) using the TaKaRa One Step RNA PCR kit (AMV, TaKaRa Bio Inc., Japan) and then DNA fragments were amplified using the TaKaRa Ex Taq Hot Start Version (TaKaRa Bio Inc, Japan) with the following primer sets. A total of 1065 bp of the polymerase (*pol*) fragment (HXB2: 2243–3308) containing the regions encoding the full protease and first 560 nucleotides of RT was amplified by RT-PCR with primers of F-1849 (5′-GAT GAC AGC ATG TCA GGG AG-3′) and R-3500 (5′-CTA TTA AGT CTT TTG ATG GGT CAT AA-3′). DRPRO5 (5′-AGA CAG GYT AAT TTT TTA GGG A-3′), DRPRO2L (5′-TAT GGA TTT TCA GGC CCA ATT TTT GA-3′), DRRT1L (5′-ATG ATA GGG GGA ATT GGA GGT TT-3′), and DRRT4L (5′-TAC TTC TGT TAG TGC TTT GGT TCC-3′) primer sets were used for nested PCR. A total of 447 bp of the envelope (*env*) fragment (HXB2: 6834–7281) containing the region C2V3 was amplified by RT-PCR with primers of V1V2-1 (5′-TGT GTA CCC ACA GAC CCC AAC CC-3′) and IC462M (5′-GCC CAT AGT GCT TCC TGC TGC T-3′). ENV02 (5′-ATG GTA GAA CAG ATG CAT GA-3′) and E115 (5′-AGA AAA ATT CCC CTC CAC AAT TAA-3′) primer sets were used for nested PCR. The amplified DNA was purified using the QIAquick PCR purification kit (Qiagen Inc.) according to the protocol provided by the manufacturer. Purified DNA was sequenced by using the ABI BigDye Terminator v3.1 cycle sequencing ready reaction kit (Applied Biosystems, Foster City, CA) and processed with an automated ABI 3730 DNA Analyzer (Applied Biosystems).

HIV-1 subtype determination and distance-based phylogenetic inference

Analyses of HIV-1 subtype and circulating recombinant form were performed using the REGA HIV-1 Subtyping Tool.[7] The basic local alignment search tool (BLAST) (www.ncbi.nlm.nih.gov/BLAST) was used to search and select the HIV-1 reference sequences with the highest similarity score (>95%) to the Mongolian strains. Additional reference

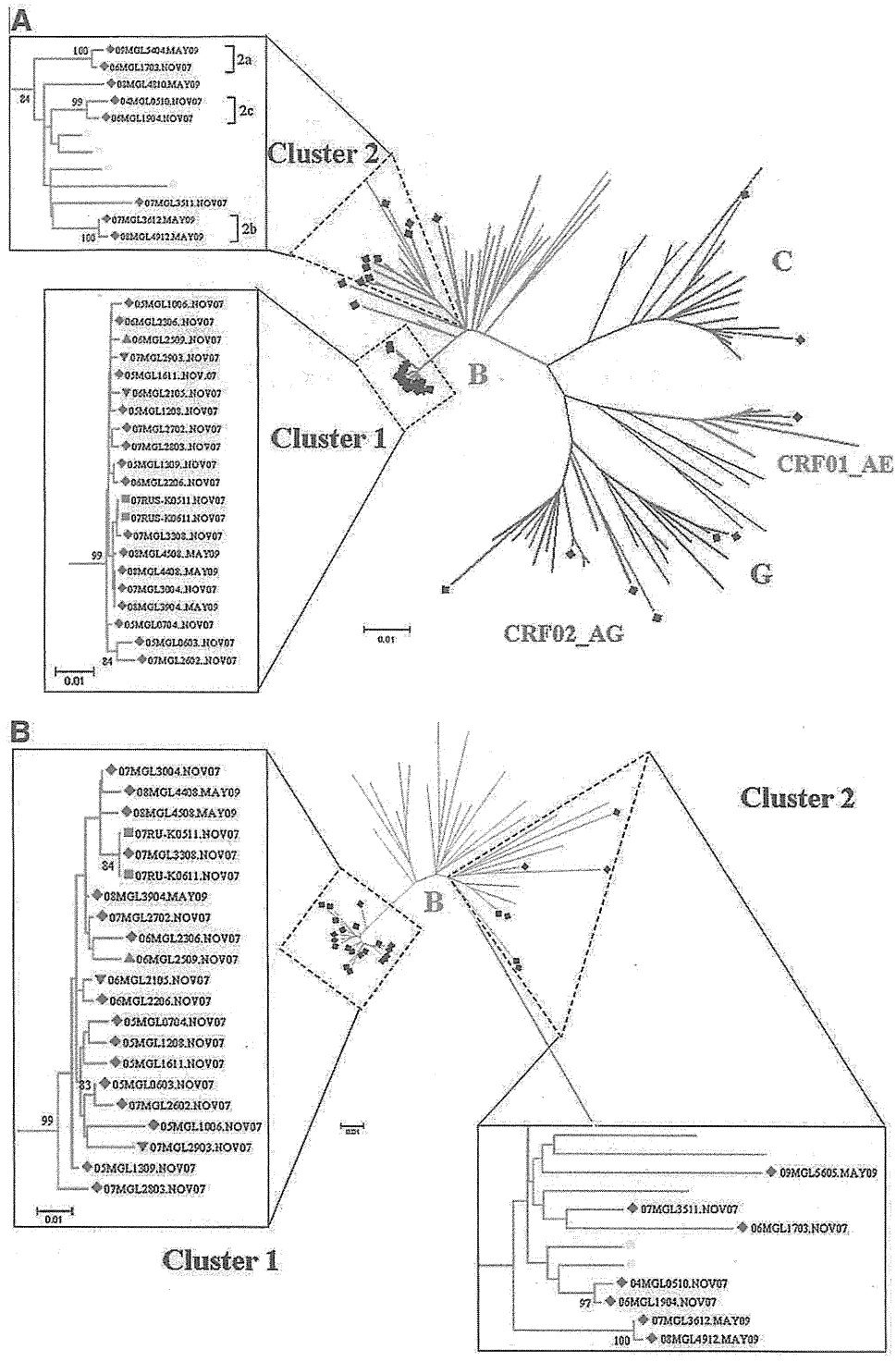

FIG. 1. Distance-based phylogenetic tree. Unrooted radial phylogeny of (A) 41 tested sequences and 67 reference HIV-1 *pol* (PR to RT; 1065 nt) sequences with different subtypes; (B) 28 tested sequences and 21 reference HIV-1 subtype B *env* (C2V3; 447 nt) sequences. The color of the branches represents the different subtypes and recombinant forms. *Solid diamonds:* sequences from Mongolians. The clustered sequences are framed and subtrees of the clusters are represented in the rectangle panels on the left. Numbers on the branch in the subtrees represent bootstrap probabilities. The different symbols and different colors in the subtrees indicate risk factors and/or countries of origin of sequences [*blue diamonds:* MSM (men who have sex with men); *green triangles:* HSM (heterosexual male); *pink triangle:* HSF (heterosexual female) for Mongolians only; *red squares:* sequences isolated from Russian patients; *yellow squares:* reference sequences of Korean origin].

sequences of different subtypes and recombinant forms were retrieved from the Los Alamos National Laboratory (www.hiv.lanl.gov). Sequences were aligned using the CLUSTAL-W software in the MEGA (molecular evolutionary genetics analysis) version 4.1.[8] Phylogenetic trees were constructed by the neighbor-joining (NJ) method based on the Maximum Composite Likelihood distance matrix listed in the MEGA software. The reliabilities of the branching patterns were tested by bootstrap analysis with 1000 replicates.

Bayesian coalescent inference using the subtype B sequences

Evolutionary rates, molecular clock phylogenies, and other evolutionary parameters were estimated from heterochronous genomic sequences of subtype B in Mongolian, non-Mongolian, and some reference sequences by using the Bayesian Markov chain Monte Carlo (MCMC) method. The reference sequences were obtained from the HIV sequence

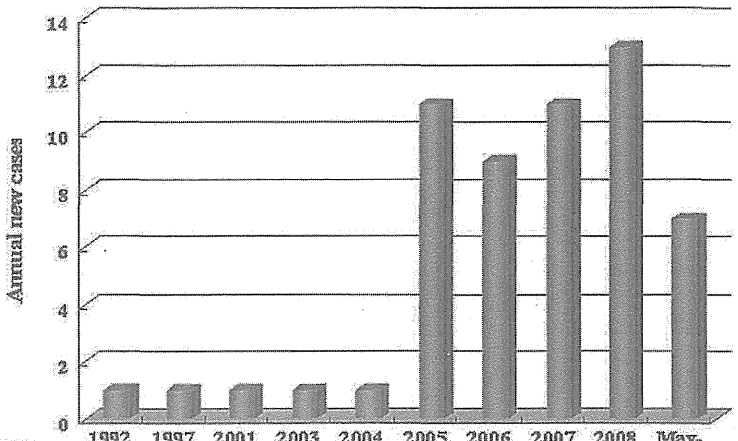

HIV-1 Subtype	1992	1997	2001	2003	2004	2005	2006	2007	2008	May-09
B (Cluster 1)						6	4	6	3	
B (Cluster 2)					1		2	2	2	1
B									2	1
C						1	1			
G									1	1
CRF01_AE								1		
CRF02_AG		1				1		2		
Unavailable	1		1	1		3	2		5	4
Total	1	1	1	1	1	11	9	11	13	7

FIG. 2. Year-diagnosis rates of HIV-1 infection in Mongolia between 1992 and May 2009 (upper panel). The number of patients and their identified HIV-1 subtypes are listed in the lower panel.

database in the Los Alamos National Laboratory with their sampling time. The reference alignment set for the *pol* region consists of 22 sequences of subtype B viruses covering Korea, China, Japan, Russia, Europe, and North America, with the sequence of D.KE.97.ML415_2 as the subtype's outgroup. The set for the *env* region consists of 20 sequences of subtype B viruses covering Korea, China, Japan, Russia, Europe, and North America, with the sequence of C.US.98US_MSC5016 as the subtype's outgroup. Each reference set was piled up with the Mongolian sequence analyzed in the present study and realigned using CLUSTAL-W. The following analyses were performed in each region of the sequence alignment. The nucleotide substitution model used in the analyses was evaluated by the hierarchical likelihood ratio test using PAUP v4.0 beta[9] with MrModel test,[10] and the general time-reversible (GTR) model[11] with both invariant sites (I) and gamma-distributed site heterogeneity (G) with four rate categories had maximum likelihood. Bayesian MCMC analyses were performed by BEAST v1.4.8[12] using the GTR+I+G and a relaxed molecular clock model (the uncorrelated lognormal-distributed model).[13] Three different population dynamic models, Exponential growth, Logistic growth, and Bayesian Skyline Plot (BSP), were tested in the analyses, and the exponential model was adopted as the most likely phylogeny according to the BSP property. Each Bayesian MCMC analysis was run for 30 million states and sampled every 10,000 states. Posterior probabilities were calculated with a burn-in of 4 million states and checked for convergence using Tracer v1.4. The maximum clade credibility tree for the analyzed set of the MCMC data was annotated by TreeAnotator in the BEAST package. The posterior distribution of the substitution rate obtained from the heterochronous sequences was subsequently incorporated as a prior distribution for evolutionary rate of the *pol* region as well as the *env* region, thereby adding a timescale to the phylogenetic histories of the given viruses and enabling the estimation of the times of the most recent common ancestors (tMRCA).[14]

Results

The *pol* region (1065 bp) was successfully amplified and sequenced in 41 sera. According to the REGA HIV-1 Subtyping Tool, the distribution of HIV-1 genotypes in the study population was as follows: 32 cases (78%) of subtype B, two (4.9%) subtype C, two (4.9%) subtype G, four (9.8%) CRF02_AG, and one case (2.4%) of CRF01_AE.

To investigate the geographic origin of the Mongolian strains, the 41 *pol* sequences were compared against all HIV-1 sequences in the NCBI database using a BLAST similarity search. A distance-based phylogenetic tree (NJ tree) was constructed with 67 *pol* reference sequences (Fig. 1A). As shown in the phylogenetic tree of the *pol* gene region, the majority (78%) of the sequences belonged to subtype B, in which two distinct clusters, named cluster 1 and cluster 2, were identified. Twenty-one (65.6%) of the total 32 subtype B sequences, which included 16 MSM, two HSM, and one HSF Mongolians, were grouped into "cluster 1." This cluster showed a remarkable monophyly with a long branch against the other sequences and high bootstrap value (<98%). The mean nucleotide diversity within the cluster was low (<0.01), indicating that members of this cluster were closely related. Russian B strains (07RUS-K0511NOV07 and 07RUS-K0611NOV07) were included in cluster 1, suggesting a Russian carrier was responsible for the Mongolian HIV-1 epidemic. Cluster 2 consisted of sequences from eight (25%) MSM Mongolian patients and four reference strains from Korean subtype B origin. Cluster 2 was more divergent than cluster 1, and had a relatively low bootstrap value (<90%). We also identified three small groups, group 2a, 2b, and 2c, in cluster 2. They had high clade credibility (bootstrap value >98%) and low genetic divergences (<0.01).

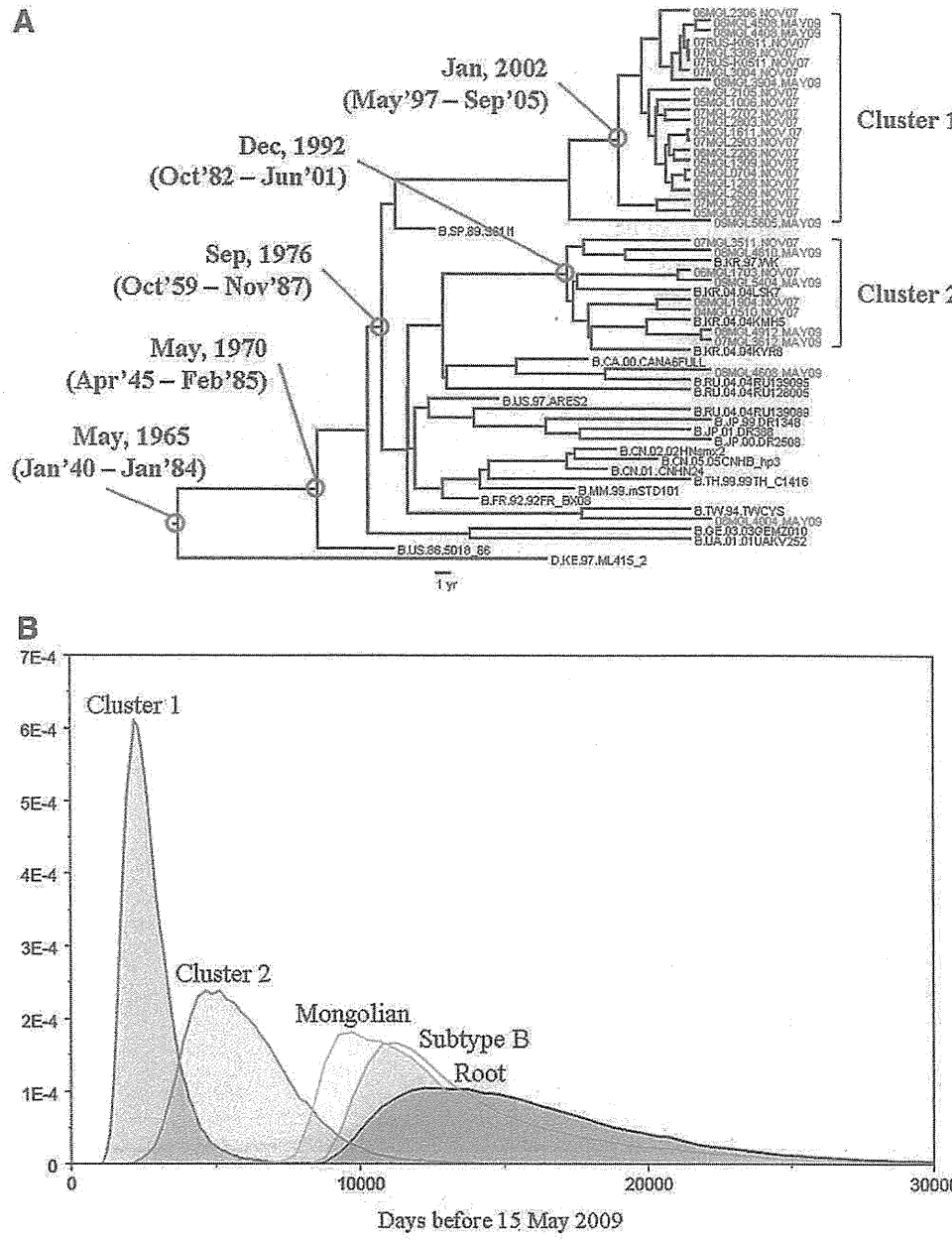

FIG. 3. Bayesian coalescence analysis of *pol* gene HIV-1 subtype B. (A) Maximum clade credibility tree of the *pol* gene by Bayesian Markov chain Monte Carlo (MCMC) analysis. The rooted tree illustrates the chronological phylogenetic relationship of 30 Mongolians and 22 reference HIV-1 subtype B *pol* (PR to RT; 1065 nt) sequences. The branch length of phylogeny is in units of time, and a yearly scale is shown under the tree. Red-purple sequence names represent the sequences in Mongolian and Russian patients, respectively. The clusters detected in the neighbor-joining (NJ) trees are annotated by brackets on the right of the tree. Month and year labels with red lines and circles indicate times of the most recent common ancestors (tMRCAs) of corresponding monophyletic groups, and the labels in parentheses indicate the 95% highest posterior density (HPD) interval of the tMRCA. (B) Marginal densities of tMRCAs on the Bayesian MCMC analysis. Blue, red, orange, green, and black represent the distribution of tMRCA estimates of cluster 1, 2, whole Mongolian subtype B, subtype B, and root height, respectively.

Two sequences isolated from two Mongolian heterosexual men belonged to subtype G. They were close relatives and seemed to have diverged from the reference sequences of subtype G of Central African (Nigeria) origin. All other remaining Mongolian sequences were from female patients. Two sequences (one was FSW) were close to the reference sequences subtype C of Asian (India) and Northeast African (Ethiopia and Burundi) origins, respectively. The sequences of four sex workers represented CRF02_AG. These sequences were close to reference strains isolated from Uzbekistan, Cameroon, and Ghana. The remaining isolated sequence was CRF01_AE, which was close to reference strains from Vietnam.

Twenty-eight out of the 32 subtype B samples based on the *pol* gene sequences were successfully amplified and the *env* (C2V3) gene region was sequenced and a phylogenetic tree was constructed (Fig. 1B). All samples were also classified as subtype B, indicating that they were not intersubtype recombinant forms if judged from the *pol* and *env* genes. Since the *env* gene region of HIV-1 has high sequence diversity, it is suitable for gene evolution analysis. Nevertheless, the intragroup nucleotide diversity of all 21 sequences on the *env* gene region in cluster 1 was very low, reflecting the rapid expansion of transmission of this lineage of HIV-1 in Mongolia. In contrast, seven other sequences on the *env* gene region belonging to cluster 2 were considerably divergent, suggesting a multiple origin of cluster 2.

Newly diagnosed cases of HIV-1 infection in Mongolia markedly increased in 2005 (Fig. 2, upper panel). Since that year, 7–13 new cases of HIV-1 infection had been diagnosed annually. Although the dominant subtype in Mongolia is currently subtype B, the first subtype-confirmed case in our analysis was CRF02_AG and was detected in 1997 (Fig. 2, lower panel). In 2004, one virus was classified into subtype B.

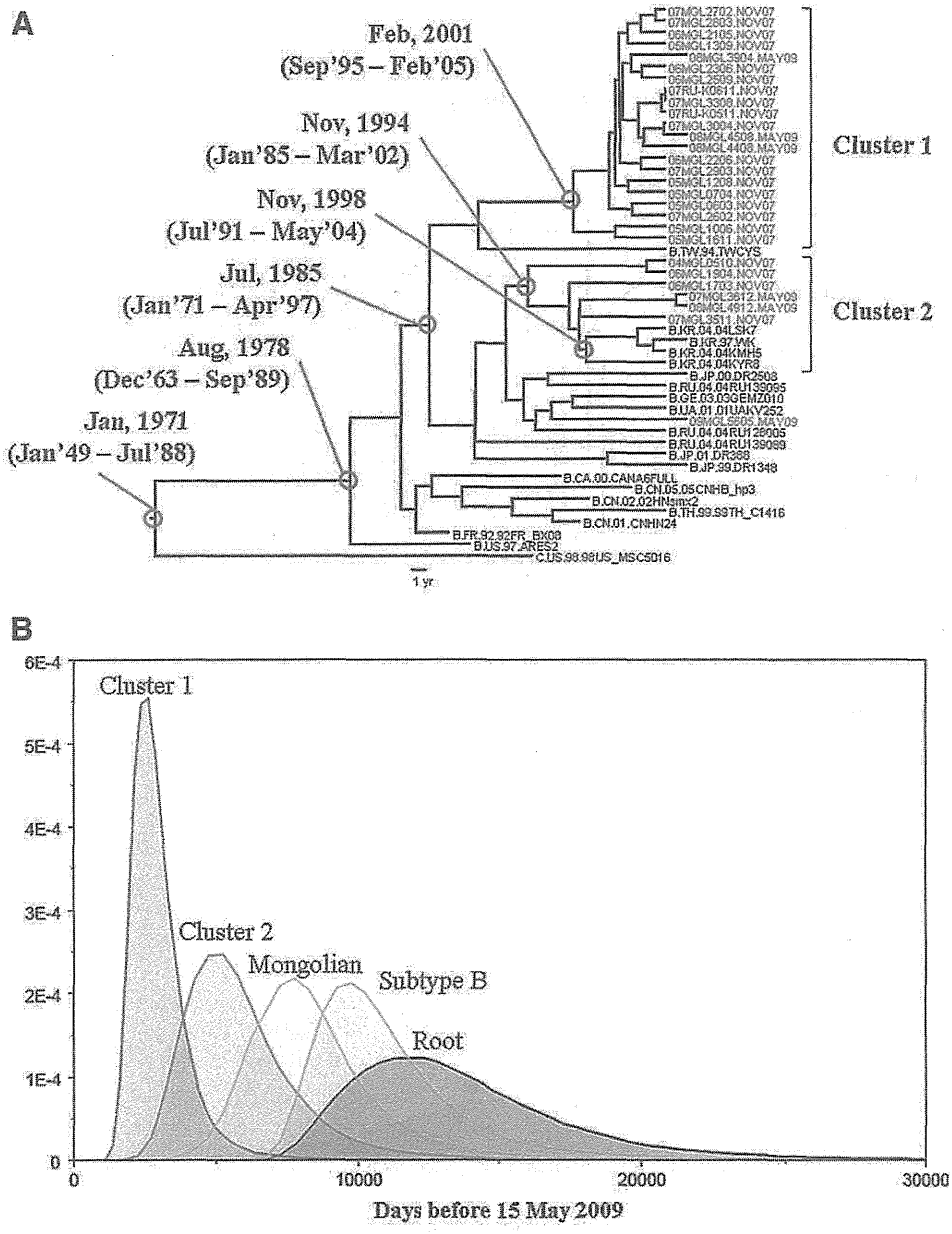

FIG. 4. Bayesian coalescence analysis of the *env* gene of subtype B. **(A)** Maximum clade credibility tree of the *env* gene by Bayesian MCMC analysis. The rooted tree illustrates the chronological phylogenetic relationship of 26 Mongolians and 23 reference HIV-1 subtype B *env* (C2V3; 447 nt) sequences. The branch length of the phylogeny is in units of time, and a yearly scale is shown under the tree. Red-purple sequence names represent the sequences of Mongolian and Russian patients, respectively. The clusters detected in the NJ trees are annotated by brackets on the right of the tree. Month and year labels with red lines and circles indicate tMRCAs of the corresponding monophyletic groups, and the labels in parentheses indicate 95% HPD confidence interval of the tMRCA. **(B)** Marginal densities of tMRCAs on the Bayesian MCMC analysis. Blue, red, orange, green, and black represent the distribution of tMRCA estimates of cluster 1, 2, whole Mongolian subtype B, subtype B, and root height, respectively.

This virus belonged to cluster 2, and was assumed to be of Korean origin. In 2005, viruses from six patients were classified as subtype B while one was subtype C and CRF02_AG, respectively. All subtype B viruses belonged to cluster 1 in our phylogenetic analysis. In 2006, viruses from six patients were also classified as subtype B, and two of them belonged to cluster 2. One of these cluster 2 viruses was also assumed to be of Korean origin (i.e., group 2c). From 2006, cluster 1 viruses had been twice as dominant as cluster 2 viruses. Other subtypes and CRFs were rarely collected in Mongolia.

To assess the result of the distance-based analysis, and to estimate tMRCAs of the Mongolian clusters, we performed a Bayesian coalescent-based phylogenetic inference. Appling the Bayesian relaxed molecular clock method to the phylogeny, the estimated mean evolutionary rates per year per site were 1.90×10^{-3} and 6.66×10^{-3} for *pol* and *env*, respectively (Supplementary Table S1; Supplementary Data are available online at www.liebertonline.com/aid). The estimated mean coefficients of variation were 0.72 and 0.48 for *pol* and *env*, indicating substantial heterogeneity in the evolutionary rate among viral lineage (Supplementary Table S1). The topology of the maximum clade credibility trees of both regions by the Bayesian MCMC analysis was similar to the NJ trees (Figs. 3 and 4), although some differences were observed between trees on the *pol* and *env* regions. One of these differences was found in Korean subtype B sequences in cluster 2. Thus, the Korean sequences formed a monophyletic group in the *pol* tree, but not in the *env* tree. Another notable difference was 09MGL5605.MSM.MAY09, which was close to cluster 1 in the *pol* tree but was related to cluster 2 in the *env* tree. The remaining differences were caused by differences in the samples used for analysis; while we were able to sequence 26 samples for the *env* region, 30 sequences were available for the *pol* region. The Bayesian chronological phylogenies showed that cluster 2 had older ancestors than cluster 1. Based on the estimates of the evolutionary rate, the mean tMRCA of cluster 1

was dated January 2002 on the *pol* region (Fig. 3A) and February 2001 on the *env* region (Fig. 4A). The marginal density of the posterior probabilities of tMRCA in both regions indicated that tMRCA of cluster 1 viruses ranged from 1995 to 2005 (Figs. 3B and 4B). On the other hand, the mean tMRCA of cluster 2 was dated December 1992 on the *pol* region (Fig. 3A) and November 1994 on the *env* region (Fig. 4A). The marginal density of tMRCA of cluster 2 was blunter than that of cluster 1, showing less reliability of tMRCA estimates of cluster 2. The root height of all Mongolian and U.S.-related subtype B reference sequences dated from the late 1960s to early 1970s.

Discussion

It is important to monitor circulating subtypes and the emerging genetic diversity of HIV-1 not only because it has implications for global surveillance but also because it should facilitate risk analysis of HIV-1 transmission and help effective strategies for HIV-1 prevention.[15–19]

The present study is the first report that provides definitive evidence of HIV-1 infection occurring in a low prevalence country, Mongolia. Our results showed that HIV-1 subtype B is responsible for nearly 78% of the analyzed samples, and possibly by sexual network within the predominant MSM (84.8%) risk group. The phylogenetic analyses of HIV-1 *pol* subtype B sequences from Mongolian and non-Mongolian origins showed that sequences of cluster 1 and cluster 2 formed monophyletic groups compared with other viruses of the same and different subtypes from around the world, indicating that HIV-1 subtype B entered Mongolia through two distinct origins.

The most intriguing feature of this epidemic is the very low genetic diversity of cluster 1. Molecular analysis strongly indicated that HIV-1 spread rapidly during a relatively short period with the same ancestor virus. Patients of cluster 1 were diagnosed between 2005 and 2008. However, the result of the Bayesian MCMC analyses suggests that the main outbreak occurred around the early 2000s. The short-term expansion also strongly suggests a high-risk sexual behavior in this population.[20] Although most patients were MSM, the group also included bisexual and female patients. They could potentially serve as a bridge between MSM and a lower-risk population, such as heterosexually active adults. Based on the extremely high prevalence of syphilis in FSW as determined in our nationwide surveillance of HIV/STI in 2007,[2] Mongolia is at high risk of an expansion of HIV-1 infection. In Russia, subtype B is not a major subtype in the total HIV epidemic but is predominant among MSM.[21] However, it is possible that the Russian subtype B strain may become the major strain in the Mongolian population in the future. Based on this, comprehensive preventive measures are urgently needed for this group and our team has already started taking action.

The median evolution rates estimated for Mongolian subtype B in the *pol* (1.9×10^{-3} substitution site per year) and *env* region (6.66×10^{-3} substitution site per year) were comparable with the rates reported previously for these genomic regions for subtype B in other countries (*pol* 2.5×10^{-3} substitution site per year,[22] *env* $5–7\times10^{-3}$ substitution site per year[23,24]). Considering these evolutionary rates, the older origin was probably from Korean HIV-1 subtype B, and first emerged in Mongolia around the early 1990s, almost a decade before the first detection of HIV-1 subtype B in Mongolia. However, this group also has the potential to be a major cluster in the future. This conclusion is based on the demographic data that documented that most of the patients in this group lived in South Korea as migrant workers. At present, more than 10,000 Mongolian migrant workers live and work in South Korea. They are usually young, sexually active, and living alone. Their working and living conditions are unstable and looking for friends and sex partners is not easy in a new environment. Given these circumstances, these workers are a vulnerable population for HIV-1 infection. These data clearly demonstrate that education on HIV-1 infection among the migrant workers is not enough and comprehensive actions for the prevention of HIV-1 infection are needed before these workers go abroad.

In conclusion, our study identified a hot spot of HIV-1 transmission expanding currently and the potential seed of the epidemic in Mongolia. Comprehensive preventive measures are crucial to keep the rate of HIV-1 infection low in Mongolia. Our study provided clues for effective strategic actions for HIV-1 prevention.

Acknowledgments

This study was supported by grants from the National Center for Global Health and Medicine (H20-04-R) from the Ministry of Health, Labour, and Welfare of Japan and from the Global Center of Excellence Program (Global Education and Research Center Aiming at the Control of AIDS) from the Ministry of Education, Science, Sports, and Culture of Japan. The authors would like to thank all the doctors and assistant nurses of the AIDS/STI Department NCCD, Mongolia, for their roles in enrolling study participants and collecting blood samples. We are also grateful to all participants who contributed to the study.

Author Disclosure Statement

No competing financial interests exist.

References

1. Ministry of Health Mongolia, Global Fund supported project on AIDS and TB: Second generation HIV/STI surveillance report–2007. Mongolia, 2007.
2. Davaalkham J, Unenchimeg P, Baigalmaa Ch, *et al.*: High-risk status of HIV-1 infection in the very low epidemic country, Mongolia, 2007. Int J STD AIDS 2009;20:391–394.
3. Bello G, Passaes CP, Guimarães ML, *et al.*: Origin and evolutionary history of HIV-1 subtype C in Brazil. AIDS 2008;22:1993–2000.
4. Gilbert MT, Rambaut A, Wlasiuk G, *et al.*: The emergence of HIV/AIDS in the Americas and beyond. Proc Natl Acad Sci USA 2007;104:18566–18570.
5. Worobey M, Gemmel M, Teuwen DE, *et al.*: Direct evidence of extensive diversity of HIV-1 in Kinshasa by 1960. Nature 2008;455:661–664.
6. Salemi M, de Oliveira T, Ciccozzi M, *et al.*: High-resolution molecular epidemiology and evolutionary history of HIV-1 subtypes in Albania. PLoS One 2008;3:e1390.
7. de Oliveira T, Deforche K, Cassol S, *et al.*: An automated genotyping system for analysis of HIV-1 and other microbial sequences. Bioinformatics 2005;21:3797–3800.
8. Tamura K, Dudley J, Nei M, and Kumar S: MEGA4: Molecular Evolutionary Genetics Analysis (MEGA) software version 4.0. Mol Biol Evol 2007;24:1596–1599.

9. Swofford DL: PAUP*. Phylogenetic Analysis Using Parsimony (*and Other Methods). Version 4. Sinauer Associates, Sunderland, Massachusetts, 2003.
10. Nylander JAA: MrModeltest v2. Program distributed by the author. Evolutionary Biology Centre, Uppsala University, 2004.
11. Rodríguez F, Oliver JL, Marín A, *et al.:* The general stochastic model of nucleotide substitution. J Theor Biol 1990;142:485–501.
12. Drummond AJ and Rambaut A: BEAST: Bayesian evolutionary analysis by sampling trees. BMC Evol Biol 2007; 7:214.
13. Drummond AJ, Ho SY, Phillips MJ, *et al.:* Relaxed phylogenetics and dating with confidence. PLoS Biol 2006;4:e88.
14. Pybus OG, Drummond AJ, Nakano T, *et al.:* The epidemiology and iatrogenic transmission of hepatitis C virus in Egypt: A Bayesian coalescent approach. Mol Biol Evol 2003;20:381–387.
15. Bennett D: HIV [corrected] genetic diversity surveillance in the United States. J Infect Dis 2005;192:4–9.
16. de Oliveira T, Pybus OG, Rambaut A, *et al.:* Molecular epidemiology: HIV-1 and HCV sequences from Libyan outbreak. Nature 2006;444:836–837.
17. Hu DJ, Dondero TJ, Rayfield MA, *et al.:* The emerging genetic diversity of HIV. The importance of global surveillance for diagnostics, research, and prevention. JAMA 1996;275: 210–216.
18. Hué S, Clewley JP, Cane PA, *et al.:* HIV-1 pol gene variation is sufficient for reconstruction of transmissions in the era of antiretroviral therapy. AIDS 2004;18:719–728.
19. Peeters M, Toure-Kane C, and Nkengasong JN: Genetic diversity of HIV in Africa: Impact on diagnosis, treatment, vaccine development and trials. AIDS 2003;17:2547–2560.
20. Maljkovic Berry I, Ribeiro R, Kothari M, *et al.:* Unequal evolutionary rates in the human immunodeficiency virus type 1 (HIV-1) pandemic: The evolutionary rate of HIV-1 slows down when the epidemic rate increases. J Virol 2007;81:10625–10635.
21. Bobkov AF, Kazennova EV, Selimova LM, *et al.:* Temporal trends in the HIV-1 epidemic in Russia: Predominance of subtype A. J Med Virol 2004;74:191–196.
22. Hué S, Pillay D, Clewley JP, *et al.:* Genetic analysis reveals the complex structure of HIV-1 transmission within defined risk groups. Proc Natl Acad Sci USA 2005;102:4425–4429.
23. Leitner T and Albert J: The molecular clock of HIV-1 unveiled through analysis of a known transmission history. Proc Natl Acad Sci USA 1999;96:10752–10757.
24. Robbins KE, Lemey P, Pybus OG, *et al.:* U.S. human immunodeficiency virus type 1 epidemic: Date of origin, population history, and characterization of early strains. J Virol 2003;77:6359–6366.

Address correspondence to:
Davaalkham Jagdagsuren
AIDS Clinical Center
National Center for Global Health and Medicine
1-21-1, Toyama, Shinjuku-ku
Tokyo 162-8655
Japan

E-mail: jdavaalkham@yahoo.com

K70Q Adds High-Level Tenofovir Resistance to "Q151M Complex" HIV Reverse Transcriptase through the Enhanced Discrimination Mechanism

Atsuko Hachiya[1,2], Eiichi N. Kodama[3]*, Matthew M. Schuckmann[1], Karen A. Kirby[1], Eleftherios Michailidis[1], Yasuko Sakagami[4], Shinichi Oka[2], Kamalendra Singh[1], Stefan G. Sarafianos[1]*

1 Department of Molecular Microbiology and Immunology, University of Missouri School of Medicine, Columbia, Missouri, United States of America, **2** AIDS Clinical Center, National Center for Global Health and Medicine, Tokyo, Japan, **3** Division of Emerging Infectious Diseases, Tohoku University School of Medicine, Sendai, Japan, **4** Institute for Virus Research, Kyoto University, Kyoto, Japan

Abstract

HIV-1 carrying the "Q151M complex" reverse transcriptase (RT) mutations (A62V/V75I/F77L/F116Y/Q151M, or Q151Mc) is resistant to many FDA-approved nucleoside RT inhibitors (NRTIs), but has been considered susceptible to tenofovir disoproxil fumarate (TFV-DF or TDF). We have isolated from a TFV-DF-treated HIV patient a Q151Mc-containing clinical isolate with high phenotypic resistance to TFV-DF. Analysis of the genotypic and phenotypic testing over the course of this patient's therapy lead us to hypothesize that TFV-DF resistance emerged upon appearance of the previously unreported K70Q mutation in the Q151Mc background. Virological analysis showed that HIV with only K70Q was not significantly resistant to TFV-DF. However, addition of K70Q to the Q151Mc background significantly enhanced resistance to several approved NRTIs, and also resulted in high-level (10-fold) resistance to TFV-DF. Biochemical experiments established that the increased resistance to tenofovir is not the result of enhanced excision, as K70Q/Q151Mc RT exhibited diminished, rather than enhanced ATP-based primer unblocking activity. Pre-steady state kinetic analysis of the recombinant enzymes demonstrated that addition of the K70Q mutation selectively decreases the binding of tenofovir-diphosphate (TFV-DP), resulting in reduced incorporation of TFV into the nascent DNA chain. Molecular dynamics simulations suggest that changes in the hydrogen bonding pattern in the polymerase active site of K70Q/Q151Mc RT may contribute to the observed changes in binding and incorporation of TFV-DP. The novel pattern of TFV-resistance may help adjust therapeutic strategies for NRTI-experienced patients with multi-drug resistant (MDR) mutations.

Citation: Hachiya A, Kodama EN, Schuckmann MM, Kirby KA, Michailidis E, et al. (2011) K70Q Adds High-Level Tenofovir Resistance to "Q151M Complex" HIV Reverse Transcriptase through the Enhanced Discrimination Mechanism. PLoS ONE 6(1): e16242. doi:10.1371/journal.pone.0016242

Editor: Zandrea Ambrose, University of Pittsburgh, United States of America

Received September 15, 2010; **Accepted** December 8, 2010; **Published** January 13, 2011

Funding: This work was supported by a grant for the promotion of AIDS Research from the Ministry of Health, Labor and Welfare (AH and EK, http://www.mhlw.go.jp/english/index.html), by grants from the Korea Food & Drug Administration and the Ministry of Knowledge and Economy, Bilateral International Collaborative R&D Program, Republic of Korea (SGS) and by National Institutes of Health (NIH, http://nih.gov/) research grants AI094715, AI076119, AI079801, and AI074389 to SGS. The funders had no role in study design, data collection and analysis, decision to publish, or preparation of the manuscript.

Competing Interests: The authors have declared that no competing interests exist.

* E-mail: sarafianoss@missouri.edu (SGS); kodama515@m.tains.tohoku.ac.jp (ENK)

Introduction

Nucleos(t)ide reverse transcriptase inhibitors (NRTIs) are used in combination with other classes of drugs for the treatment of patients infected with human immunodeficiency virus type-1 (HIV-1). This approach is known as highly active anti-retroviral therapy (HAART) and has been remarkably successful in reducing the viral loads and increasing the number of CD4+ cells in patients' plasma. However, prolonged therapies inevitably result in resistance to all of the available drugs. Several mutations in the reverse transcriptase (RT) are known to cause resistance to NRTIs through two basic mechanisms:

1) The excision mechanism, which is based on an enhanced capacity of RT to use adenosine triphosphate (ATP) as a nucleophile for the removal of the chain-terminating nucleotide from the DNA terminus. The excision reaction products are a 5′, 5′-dinucleoside tetraphosphate and an unblocked primer with a free 3′-OH, allowing DNA synthesis to resume [1,2,3]. Increased excision of NRTIs is imparted by Excision Enhancement Mutations, typically M41L, D67N, K70R, T215Y/F, L210W, and K219E/Q (also known as Thymidine Associated Mutations, or TAMs). Other mutations have also been reported to enhance excision, including insertions or deletions at the tip of the β3- β4 loop of the fingers subdomain in the background of other excision enhancement mutations [4,5,6,7,8,9,10,11].

2) The other mechanism of NRTI resistance is the exclusion mechanism, which is caused when NRTI-resistance mutations in RT enhance discrimination and reduce incorporation of the NRTI-triphosphate (NRTI-TP). This mechanism is exemplified by the resistance of the M184V RT mutant to lamivudine (3TC) and emtricitabine (FTC) due to steric clash between the β-branched Val or Ile at position 184 and the oxathiolane ring of the inhibitors [12,13]. Another example of the exclusion mechanism is the multi-drug resistant (MDR) HIV-1 RT known as Q151M complex (Q151Mc). This RT contains the Q151M mutation together with a cluster of four

additional mutations (A62V/V75I/F77L/F116Y) [14,15]. Q151M by itself causes intermediate- to high-level resistance to zidovudine (AZT), didanosine (ddI), zalcitabine (ddC), stavudine (d4T), and low level resistance to abacavir (ABC) [15,16,17] without reducing viral fitness [18,19]. Addition of the four associated mutations increases replication capacity of RT and results in high-level resistance to AZT, ddI, ddC, and d4T, 5-fold resistance to ABC and low-level resistance to lamivudine (3TC) and emtricitabine (FTC) [17,18,19,20,21]. Miller *et al.* and Smith *et al.* reported a 1.8-fold and 3.6-fold increase in resistance to tenofovir (TFV), respectively [22,23].

Biochemical studies on the mechanism of Q151Mc resistance to multiple NRTIs have revealed that the mutations of this complex decrease the maximum rate of NRTI-TP incorporation without significantly affecting the incorporation of the natural nucleotides [21,24,25]. Structurally, the Q151 residue interacts with the 3′-OH of a normal deoxynucleoside triphosphate (dNTP) substrate [26]. It appears that the Q151Mc mutations cause resistance to multiple NRTIs by affecting the hydrogen bond network involving protein side chains in the vicinity of the dNTP-binding site and the NRTI triphosphate lacking a 3′-OH [25,26,27]. The Q151Mc set of mutations was also reported to decrease pyrophosphate PPi- and ATP-mediated excision [25].

K65R is another mutation near the polymerase active site that confers NRTI resistance through the exclusion mechanism. Specifically, K65R RT has reduced susceptibility to the acyclic nucleotide analog, TFV and other NRTIs, including ddI, ddC, ABC, FTC and 3TC [28,29,30,31]. Biochemical studies with K65R RT have demonstrated that this enzyme decreases the incorporation rate of these NRTIs [32,33,34]. The crystal structure of K65R RT in complex with DNA and TFV diphosphate (TFV-DP) revealed that R65 forms a molecular platform with the conserved residue R72, and the platform enhances the ability of K65R RT to discriminate NRTIs from dNTPs [35]. HIV carrying the Q151Mc mutations has been reported to be susceptible to TFV disoproxil fumarate (TFV-DF), the oral prodrug of TFV that enhances its oral bioavailability and anti-HIV activity [22,36]. While the K65R mutation appeared in several patients treated for more than 18 months with TFV-DF, no patient developed multi-NRTI resistance through appearance of Q151Mc [37].

Here we report the identification of unique HIV clinical isolates that have acquired the K70Q mutation in the background of Q151Mc during TFV-DF-containing therapy. We have used a combination of virological, biochemical, and molecular modeling methods to derive the mechanism by which this mutation confers resistance to TFV.

Materials and Methods

Clinical samples

HIV was isolated from fresh plasma immediately after collection of clinical samples from study participants at the outpatient clinic of the AIDS Clinical Center (ACC), International Medical Center of Japan. The Institutional Review Board approved this study (IMCJ-H13-80) and a written consent was obtained from all participants.

Construction of recombinant clones of HIV-1

Recombinant infectious clones of HIV-1 carrying various mutations were prepared using standard site-directed mutagenesis protocols as described previously [38]. The NL4-3-based molecular clone was constructed by replacing the *pol*-coding region with the HIV-1 BH10 strain. Restriction enzyme sites *Xma I* and *Nhe I* were introduced by silent mutations into the molecular clone at positions corresponding to HIV-1 RT codons 15 and 267, respectively [39]. Each molecular clone was transfected into COS-7 cells. Cells were grown for 48 h, and culture supernatants were harvested and stored at −80°C until use.

Single-cycle drug susceptibility assay

Susceptibilities to various RT inhibitors were determined using the MAGIC-5 cells which are HeLa cells stably transfected with a β-galactosidase gene under the control of an HIV long terminal repeat promoter, and with vectors that express the CD4 receptor and the CCR5 co-receptor under the control of the CMV promoter as described previously [40]. Briefly, MAGIC-5 cells were infected with diluted virus stock (100 blue forming units) in the presence of increasing concentrations of RT inhibitors, cultured for 48 h, fixed, and stained with X-Gal (5-bromo-4-chloro-3-indolyl-β-D-galacto-pyranoside). The stained cells were counted under a light microscope. Drug concentrations reducing the number of infected cells to 50% of the drug-free control (EC_{50}) were determined from dose response curves.

Enzymes

RT sequences coding for the p66 and p51 subunits of BH10 were cloned in the pRT dual vector, which is derived from pCDF-2 with LIC duet minimal adaptor (Novagen), using restriction sites *PpuMI* and *SacI* for the p51 subunit, and *SacII* and *AvrII* for the p66 subunit. RT was expressed in the *Escherichia coli* strain BL21 (Invitrogen) and purified by nickel affinity chromatography and MonoQ anion exchange chromatography [41]. RT concentrations were determined spectrophotometrically based on absorption at 260 nm using a calculated extinction coefficient (261,610 M^{-1} cm^{-1}). The active site concentration of the various RT preparations was calculated as described below.

Nucleic acid substrates

DNA oligomers were synthesized by Integrated DNA Technologies (Coralville, IA). An 18-nucleotide DNA primer fluorescently labeled with Cy3 at the 5′ end (P_{18}; 5′-Cy3 GTC CCT GTT CGG GCG CCA-3′) and a 100-nucleotide DNA template (T_{100}; 5′-TAG TGT GTG CCC GTC TGT TGT GTG ACT CTG GTA ACT AGA GAT CCC TCA GAC CCT TTT AGT CAG TGT GGA AAA TCT CTA GCA GTG GCG CCC GAA CAG GGA C-3′) were used in primer extension assays. An 18-nucleotide DNA primer 5′-labeled with Cy3 (P_{18}; 5′-Cy3 GTC ACT GTT CGA GCA CCA-3′) and a 31-nucleotide DNA template (T_{31}; 5′- CCA TAG CTA GCA TTG GTG CTC GAA CAG TGA C-3′) were used in the ATP rescue assay and pre-steady state kinetic experiments.

Active site titration and determination of the dissociation constant for DNA binding ($K_{D\text{-}DNA}$)

Determination of active site concentrations in the different preparations of WT and mutant RTs were performed using pre-steady state burst experiments. A fixed concentration of RT (80 nM, determined by absorbance measurements) was pre-incubated with increasing concentrations of DNA/DNA template/primer (T_{31}/P_{18}), followed by rapidly mixing with a reaction mixture containing $MgCl_2$ and dATP, at final concentrations of 5 mM and 50 μM, respectively. The reactions were quenched at various times (10 ms to 5 s) by adding EDTA to a final concentration of 50 mM. The amounts of product (P_{18}-dAMP) were quantitated and fit to the following burst equation:

$$P = A\left(1 - e^{-kobst}\right) + k_{ss}t \quad (1)$$

where A is the amplitude of the burst phase that represents the RT-DNA complex at the start of the reaction, k_{obs} is the observed burst rate constant for dNTP incorporation, k_{ss} is the steady state rate constant, and t is the reaction time. The rate constant of the linear phase (k_{cat}) can be estimated by dividing the slope of the linear phase by the enzyme concentration. The active site concentration and template/primer binding affinity ($K_{D\text{-}DNA}$) were determined by plotting the amplitude (A) against the concentration of template/primer. The data were fit using non-linear regression to a quadratic equation:

$$A = 0.5(K_D + [RT] + [DNA]) - \sqrt{0.25(K_D + [RT] + [DNA])^2 - ([RT][DNA])} \quad (2)$$

where K_D is the dissociation constant for the RT-DNA complex, and [RT] is the concentration of active polymerase molecules. Subsequent biochemical experiments were performed using corrected active site concentrations [42,43].

Primer extension assay

To examine the DNA polymerase activity of WT and mutant RTs and the inhibition of DNA synthesis by TFV, the primer extension assays were carried out on the T_{100}/P_{18} template/primer (P_{18} was 5′-Cy3 labeled) in the presence or absence of 3.5 mM ATP [41]. The enzyme (20 nM active sites) was incubated with 20 nM template/primer at 37°C in a buffer containing 50 mM Tris-HCl, pH 7.8 and 50 mM NaCl. The DNA synthesis was initiated by the addition of 1 μM dNTP and 10 mM $MgCl_2$. The primer extension assays were carried out in the presence or absence of varying concentrations of TFV-DP. The reactions were terminated after 15 min by adding equal volume of 100% formamide containing traces of bromophenol blue. The extension products were resolved on a 7 M urea-15% polyacrylamide gel, and visualized by phosphor-imaging (FLA 5100, Fujifilm, Tokyo). We followed standard protocols that utilize the Multi Gauge software (Fujifilm) to quantitate primer extension [41,44]. The results from dose response experiments were plotted using Prism 4 (GraphPad Software Inc., CA) and IC_{50} values for TFV-DP were obtained at midpoint concentrations.

ATP-dependent rescue assay

Template/primer (T_{31}/P_{18}) terminated with TFV (T/P_{TFV}) was prepared as described in Michailidis et al [41]. 20 nM of T/P_{TFV} was incubated at 37°C with HIV-1 RT (60 nM), either at various concentrations of ATP (0–7 mM) for 30 minutes, or for various times (0–120 minutes) with 3.5 mM ATP, in RT buffer containing 50 mM Tris-HCl, pH 7.8, and 50 mM NaCl, and 10 mM $MgCl_2$. The assay was performed in the presence of excess competing dATP (100 μM) that prevented reincorporation of the excised TFV, 0.5 μM dTTP and 10 μM ddGTP. Reactions were quenched with 100% formamide containing traces of bromophenol blue and analyzed as described above. The dissociation constants (K_d) of the various enzymes for ATP used in the rescue reactions were determined by fitting the rescue data at various ATP concentrations, using non-linear regression fitting to hyperbola.

Kinetics of dNTP incorporation by WT and mutant enzymes

To determine the binding affinity of WT and mutant enzymes to the dNTP substrate ($K_{D\text{-}dNTP}$) and to estimate the maximum rate of dNTP incorporation by these enzymes (k_{pol}), we carried out transient-state experiments using a rapid quench instrument (RQF-3, Kintek Corporation, Clarence, PA) at 37°C in RT buffer (50 mM Tris-HCl, pH 7.8 and 50 mM NaCl). HIV-1 RT (50 nM active sites) was pre-incubated with 50 nM T_{31}/P_{18} in one syringe (Syringe A), whereas varying concentrations of dNTP and 10 mM $MgCl_2$ were kept in another syringe (Syringe B). The solutions were rapidly mixed to initiate reactions, which were subsequently quenched at various times (5 ms to 10 s) by adding EDTA to a final concentration of 50 mM. The products from each quenched reaction were resolved, quantitated, and plotted as described above. The data were fit by non-linear regression to the burst equation (Eq 1).

To obtain the dissociation constant $K_{D\text{-}dNTP}$ for dNTP binding to the RT-DNA complex, the observed burst rates (k_{obs}) were fit to the hyperbolic equation (Eq. 3) using nonlinear regression:

$$k_{obs} = \left(k_{pol}[dNTP]\right)/(K_{D-dNTP} + [dNTP]) \quad (3)$$

where k_{pol} is the optimal rate of dNTP incorporation.

The kinetics of TFV incorporation by the WT and mutant enzymes were carried out in a manner similar to that employed for natural dNTP substrate except the time of reactions. It was noted that the mutant enzymes required longer time to incorporate TFV compared to the WT HIV-1 RT (detailed in the Results section).

Molecular Modeling

Molecular models of mutant enzymes were generated using SYBYL (Tripos Associates, St. Louis, MO). The starting protein coordinates were from the crystal structure of HIV-1 RT in complex with DNA template/primer and TFV-DP (PDB file 1T05) [45]. They were initially modified by the Protein Preparation tool (Schrodinger Molecular Modeling Suit, NY), which deletes unwanted water molecules, sets charges and atom type of metal ions, corrects misoriented Gln and Asn residues, and optimizes H-atom orientations. Amino acid side chains were substituted in by Maestro (Schrodinger, Molecular Modeling Suite, NY). Molecular dynamics simulations of the WT and mutant RT models were carried out to obtain the most stable structures by Impact, interfaced with Maestro at constant temperature, and OPLS_2005 force field. The molecular dynamics simulations were performed for 1000 steps with 0.001 ps intervals. The temperature relaxation time was 0.01 ps. The Verlet integration algorithm was used in simulations. The structures were imported into Pymol (http://www.pymol.org) for visualization and comparison.

Results

Phenotypic resistance to TFV-DF in the absence of any known TFV resistance mutations

During phenotypic and genotypic evaluation of the clinical isolates we identified a unique virus that exhibited an apparent discordance between the phenotypic and genotypic results. The clinical history of the patient and the corresponding genotypic and phenotypic changes during the course of the therapy are summarized in Fig. 1. (Also see Table S1). The patient's treatment before Feb 2002 included d4T, ddI, and EFV and did not decrease significantly the viral loads (Fig 1A). Hence, the therapeutic regimen was switched to TFV-DF, EFV, and the protease inhibitor lopinavir (LPV). However, the patient's immunological and virological responses still did not improve due to poor adherence, especially to LPV. Genotypic and phenotypic analyses on March 2002 (point 1) and June 2002 (point 2) revealed

A

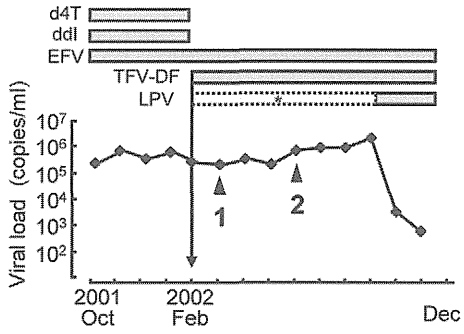

B Phenotypic profile

Isolate	Fold increase in EC_{50}								
	AZT	ddI	d4T	3TC	ABC	**TFV-DF**	FTC	NVP	EFV
1	61	12	9	13	10	**2**	9	>200	>500
2	57	>40	>50	31	15	**6**	5	>200	>500

C Genotypic profile

Isolate	Resistance-associated mutation		Other newly acquired mutations
	NRTI	NNRTI	
1	Q151M complex,	V106M, V179D	-
2	Q151M complex,	V106M, V179D, V108I	**K70Q**, K102R

Figure 1. Clinical course of patient and drug resistance profile. (A) The two clinical isolates were collected from the patient at the time points indicated by triangles. Both isolates had no known resistant mutations in the protease region. During the period indicated by asterisk, LPV was administrated but the patient demonstrated poor adherence due to undesirable side effects. After instruction on the use of antiretroviral drugs, the viral loads successfully decreased below the detection limit (<50 copies/ml). (B) Phenotypic drug susceptibility assays of clinical isolates in at least three independent experiments are shown as a relative increase in EC_{50} compared to HIV-1 NL4-3 strain which served as WT (see also Table S1). (C) Mutations observed in the isolates that are defined as the NRTI and NNRTI resistance associated mutations deposited in the HIV Drug Resistance Database maintained by International AIDS Society 2009 [58] and the Stanford University (http://hivdb.stanford.edu/) were shown. Abbreviations of drugs used: d4T, stavudine; ddI, didenosine; EFV, efavirenz; TFV-DF, tenofovir disoproxil fumarate; LPV, lopinovir; AZT, zidovudine; 3TC, lamivudine; ABC, abacavir; FTC, emtricitabine; NVP, nevirapine.
doi:10.1371/journal.pone.0016242.g001

resistance to multiple RT inhibitors, including NNRTIs (Fig 1B). Resistance to all NRTIs, except AZT and FTC, was enhanced in the point 2 isolate (Fig. 1B). Notably, this isolate showed an increase in resistance to TFV-DF in the absence of the canonical TFV resistance mutation (K65R) and in the presence of Q151Mc mutations (Fig. 1C). Previously, it has been shown that Q151Mc remains susceptible to TFV [22] although Smith *et al.* reported that Q151Mc had a 3.6-fold increase in TFV resistance [23]. Suppression of the viral load was finally achieved by improvement in drug adherence to LPV and by the addition of FTC in the therapeutic regimen, since no protease resistance mutations were found within the protease coding region.

To identify the mutation(s) responsible for the unexpected resistance to TFV-DF we sequenced the entire RT coding region at time-points 1 and 2 (Figure S1, GenBank Accession Number AB506802 and AB506803). Of the three substituted residues (70, 102, and 108) amino acids 102 and 108 are part of the structurally distinct NNRTI binding pocket [46], which can mutate during EFV-based therapeutic regimens. However, residue 70 is located in the β3-β4 hairpin loop of the p66 "fingers" subdomain of HIV-1 RT, which interacts with the incoming dNTP substrate [10,27]. Different mutations at this site have been previously implicated in NRTI resistance [47], suggesting that the observed K70Q mutation may be involved in the increased resistance to TFV-DF.

NRTI resistance enhancement by mutation at residue 70

Several mutations at position 70 of HIV-1 RT (R, G, E, T, N and Q) have been reported to the Stanford HIV-1 Drug Resistance Database (http://hivdb.stanford.edu/, accessed on Feb. 27th 2010). K70Q is rarely observed in treatment-naïve patients (0.04%), but appears more often in clinical samples from NRTI-treated patients (0.1%, $p<0.0001$ compared with the frequency of K70Q in treatment-naïve patients) but not NNRTI-treated patients. Furthermore, K70Q is observed in 0.5% of the clinical samples from patients infected with HIV-1 Q151M. There have been no previous reports on a possible role of K70Q in NRTI resistance.

To examine the effect of K70Q on drug susceptibility we generated a series of HIV variants with mutations at RT codon 70 (Figure 2A and also Table S2). The HIV-1_{K70Q} variant exhibited marginal resistance to ddI and 3TC (5- and 3.3-fold, respectively), but no significant resistance to other NRTIs. We further examined whether the mutations at residue 70 affect susceptibility to NRTIs in the Q151Mc background (Figure 2B and also Table S3). HIV-$1_{K70G/Q151Mc}$ had enhanced resistance to d4T (4.6-fold) as compared to HIV-1_{Q151Mc}. Notably, HIV-$1_{K70Q/Q151Mc}$ also showed enhanced resistance to ddI and d4T (2.4- and 4.4-fold, respectively, compared to HIV-1_{Q151Mc}). In addition, HIV-$1_{K70Q/Q151Mc}$ displayed 5-fold increased resistance to TFV-DF compared to HIV-1_{Q151Mc}. Other K70 mutations exhibited little or no resistance to TFV-DF.

Primer Extension and ATP-based Rescue Assays

As mentioned earlier, a key mechanism of NRTI resistance is the excision mechanism, which is based on the enhanced ability of NRTI-resistant enzymes to use ATP for unblocking chain-terminated primers and allow for further DNA synthesis to continue [2,3,48]. To determine whether the K70Q mutation causes TFV resistance through the excision mechanism we measured the susceptibility of WT and mutant RTs to inhibition by TFV in the presence or absence of ATP. In gel-based assays, an enhancement in excision would manifest as an increase in the production of fully extended DNA when 3.5 mM ATP is included in the extension reaction [49,50]. Our extension assays in the absence of ATP (no-excision conditions) showed that addition of the K70Q mutation to Q151Mc HIV-1 RT enhances resistance to TFV-DP. However, this enhancement is not influenced by the presence of ATP (Table 1, Fig. 3A and Figure S2A). In fact, excision enhancement due to the presence of ATP measured as [IC_{50} with ATP]/[IC_{50} without ATP] was similar for all enzymes, including the WT RT (from 2.7-fold to 2.9-fold for WT, K70Q, Q151Mc, and K70Q/Q151Mc RTs) (Table 1). Using a related type of assay, the ATP-mediated rescue assay, we compared the rates by which the WT and mutant RTs unblock TFV-terminated primers and extend products past the point of chain-termination. We find that the ATP-based rescue activity of WT RT is not slower, but 1.5-, 2.5-, and 3-fold faster than that of K70Q, Q151Mc, and K70Q/Q151Mc RTs, respectively (Fig. 3B and Figure S2B). In addition, the ATP-based rescue activity of WT RT was saturated at lower concentrations of ATP than K70Q,

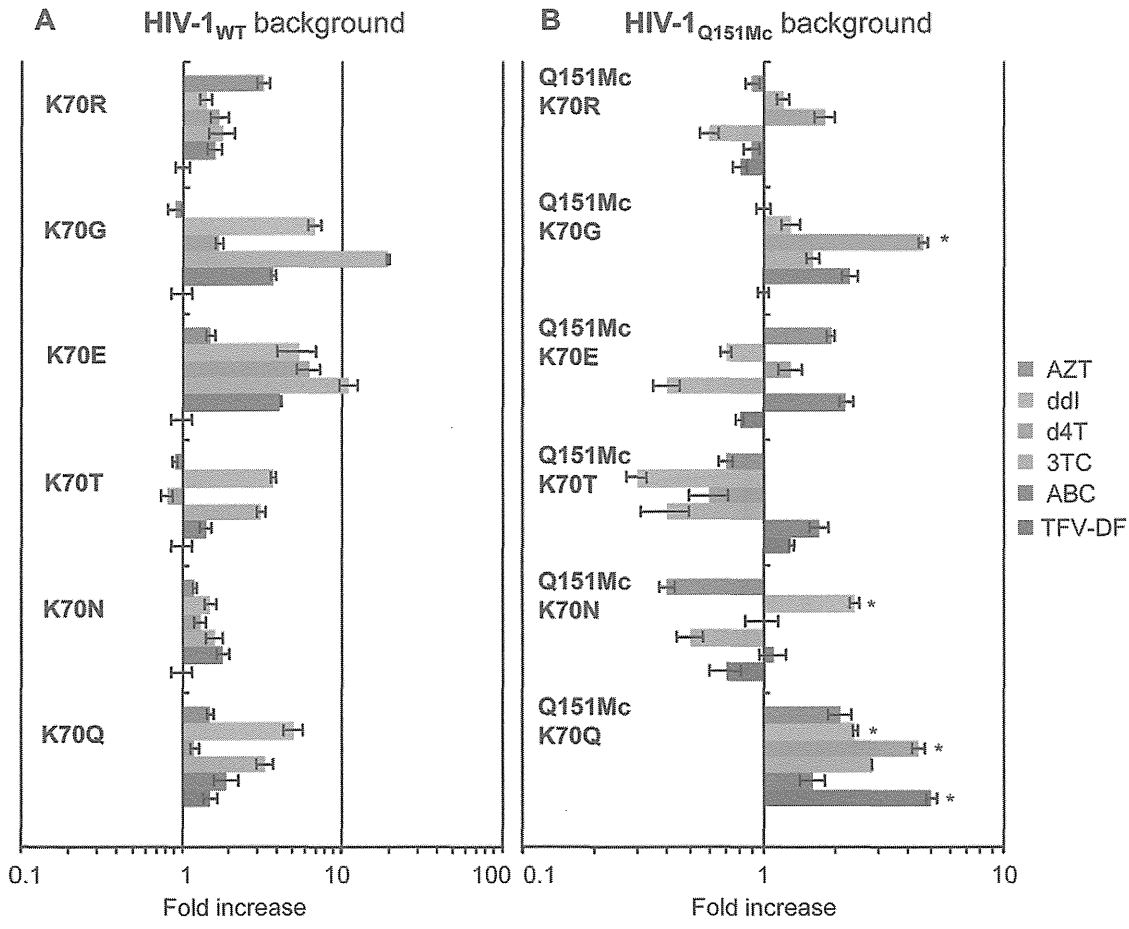

Figure 2. NRTI resistance of HIVs with mutations at RT residue 70 in the background of WT or Q151Mc. Antiviral activities of HIV-1s carrying mutations at residue 70 (K70R, K70G, K70E, K70T, K70N, or K70Q) in the WT (A) or Q151Mc (B) background were determined by the MAGIC5 assay. The data for each clone were compared to WT (A) and Q151Mc (B) HIV-1 and are shown as fold increase; AZT (red), ddI (green), d4T (cyan), 3TC (orange), ABC (blue), and TFV-DF (purple). Error bars represent standard deviations from at least three independent experiments (see also Table S2 and S3). The asterisk indicates statistically significant in EC_{50} values ($P<0.0001$ by t-test).
doi:10.1371/journal.pone.0016242.g002

Table 1. Primer extension assay in the presence or absence of ATP.

Enzyme[a]	IC_{50} (nM) of TFV-DP[b] (fold increase[c])		Excision enhancement due to ATP[d]
	Without ATP	With ATP	
WT	641±83	1854±197	2.9
	(1)[b]	(1)[b]	
K70Q	802±99	2306±270	2.9
	(1.3)	(1.2)	
Q151Mc	1503±90	3996±341	2.7
	(2.3)	(2.1)	
K70Q/Q151Mc	2392±353	7001±226	2.9
	(3.7)	**(3.8)**	

[a]The sequence of HIV RT WT and mutant derived from BH10.
[b]Data are means ± standard deviations from at least three independent experiments.
[c]The relative increase in IC_{50} value compared with each HIV-1 RT WT without, or with ATP is given in parentheses. Bold indicates an increase in fold increase value greater than 3-fold.
[d]Excision enhancement due to ATP is calculated as IC_{50} with ATP/IC_{50} without ATP.
doi:10.1371/journal.pone.0016242.t001